Journal of Medicinal Chemistry

Article

Structure-Based Design of Macrocyclic Coagulation Factor VIIa Inhibitors

E. Scott Priestley, Daniel L. Cheney, Indawati DeLucca, Anzhi Wei, Joseph M. Luettgen, Alan R. Rendina, Pancras C Wong, and Ruth Wexler

J. Med. Chem., **Just Accepted Manuscript** • DOI: 10.1021/acs.jmedchem.5b00788 • Publication Date (Web): 07 Jul 2015

Just Accepted

Journal of Medicinal Chemistry is published by the American Chemical Society. 1155 Sixteenth Street N.W., Washington, DC 20036

Structure-Based Design of Macrocyclic Coagulation Factor VIIa Inhibitors

E. Scott Priestley, Daniel L. Cheney, Indawati DeLucca, Anzhi Wei, Joseph M. Luettgen, Alan R. Rendina, Pancras C. Wong, and Ruth R. Wexler*

Bristol-Myers Squibb Research & Development, 311 Pennington-Rocky Hill Road, Pennington, NJ 08534.

RECEIVED DATE (to be automatically inserted after your manuscript is accepted if required according to the journal that you are submitting your paper to)

Running title: Macrocyclic FVIIa Inhibitors.

* To whom correspondence should be addressed. Phone: (609) 818-5756. Fax: (609) 818-3331. E-mail: scott.priestley@bms.com.

ABSTRACT. Based on a crystal structure of a phenylpyrrolidine lead and subsequent molecular modeling results, we designed and synthesized a novel series of macrocyclic FVIIa inhibitors. The optimal 16-membered macrocycle was 60-fold more potent than an acyclic analog. Further potency optimization by incorporation of P1′ alkyl sulfone and P2 methyl groups provided a macrocycle with TF/FVIIa K_i = 1.6 nM, excellent selectivity against a panel of seven serine proteases, and FVII-deficient prothrombin time EC_{2x} = 1.2 μM. Discovery of this potent, selective macrocyclic scaffold opens new possibilities for the development of orally bioavailable FVIIa inhibitors.

Introduction

The serine protease coagulation factor VIIa (FVIIa) plays a critical role in triggering the coagulation cascade. Upon vessel injury or atherosclerotic plaque rupture, the membrane-bound glycoprotein tissue factor (TF) is exposed to circulating blood containing FVIIa. The two proteins associate to form a catalytically competent complex, TF/FVIIa, which activates its substrates, Factors IX and X, leading to rapid local thrombin generation and thrombus formation.[1]

Interest in the TF/FVIIa complex as an antithrombotic drug discovery target was sparked both by the determination of its crystal structure[2] and by *in vivo* studies demonstrating the antithrombotic activity of active site inhibited FVIIa.[3, 4] Subsequent studies of small molecule FVIIa inhibitors in preclinical thrombosis and bleeding models show conclusively that inhibition of FVIIa affords excellent antithrombotic efficacy along with low bleeding liability.[5-12] Moreover, clinical trials with recombinant nematode anticoagulant protein c2, a biological agent which binds to Factor X and inhibits TF-FVIIa, demonstrate the antithrombotic efficacy and safety of this mechanism in humans.[13-15] Despite this excellent target validation, and extensive efforts to develop orally active FVIIa inhibitors from multiple chemotypes, including 2-arylbenzimidazoles,[16-22] phenylglycines,[23-26] pyrazinone and pyridone peptidomimetics,[27-31] tetrahydroquinolines,[32] fluoropyridines,[33, 34] amidinophenylureas,[35, 36] biarylacids,[37-41] α-ketoacids,[42] and phenylimidazoles,[43] amongst others, there are no reports of orally active compounds progressing into clinical trials.[44] These small molecule FVIIa inhibitors typically contain a cationic amidine group, which contributes significantly to their inhibitory potency by forming strong, bivalent hydrogen bonds with Asp189 at the bottom of the S1 pocket of FVIIa.[45] However, due to their strongly basic pKa and high polar surface area which leads to poor intrinsic membrane permeability, amidines are well known to have poor oral absorption and typically require a prodrug strategy.[10, 17, 21, 24] Alternatively, several groups have attempted to replace the amidine group in FVIIa inhibitors with less basic, more permeable alternatives,[19, 20, 22, 25, 38, 39, 41] with limited success to date, although a recent fragment screening effort has identified promising neutral S1 binders.[46] This strategy

has proven successful with inhibitors of other coagulation proteases, particularly coagulation factor Xa,[47-49] where highly optimized, potent scaffolds have enabled replacement of amidines with more permeable functional groups. Against this background, the discovery of novel FVIIa inhibitor scaffolds with high intrinsic potency is an important research goal, as it may allow replacement of the benzamidine group with a less basic, more permeable moiety to achieve oral bioavailability.

When faced with challenging protease targets, medicinal chemists now frequently employ macrocyclization as a strategy to improve the properties of their lead compounds. Macrocycles have been shown to possess improved potency,[50] selectivity,[51, 52] and pharmaceutical and pharmacokinetic properties relative to acyclic precursors.[53-56] Moreover, many macrocyclic natural products or their derivatives are in clinical use, including erythromycin, vancomycin, cyclosporin, and epothilone B, and numerous synthetically-derived macrocycles targeting HCV NS3 protease are in late stage clinical trials or have recently received regulatory approval.[57] In this report, we disclose our initial discovery of a series of rationally designed macrocycles with potent and selective inhibitory activity against FVIIa.

Design

During the course of our program to discover orally active FVIIa inhibitors, we investigated a series of phenylglycinamides containing pyrrolidine as a conformational constraint.[26] Compound **1**, containing an aminoisoquinoline P1 and an unsubstituted phenyl P2 group (Figure 1A), was found to be a potent TF/FVIIa inhibitor (TF/FVIIa K_i = 8.0 nM, FVII-deficient prothrombin time[12] EC_{2x} = 12 μM). A crystal structure with FVIIa was subsequently obtained (Figure 1B), revealing the basic 1-aminoisoquinoline group to be bound as expected in the S1 pocket, forming a salt bridge with the Asp189 side chain and a hydrogen bond with a conserved water molecule above the Tyr228 aryl ring. The central amide carbonyl oxygen is engaged in hydrogen bonds with the protonated form of the His57 imidazole ring and the Ser195 hyrdroxyl group. The P1′ and P2 phenyl rings have undergone hydrophobic collapse and are engaged in favorable van der Waals interactions in S2, specifically with the side chains of His57,

Trp215 and Thr99. The acetanilide NH engages in hydrogen bonding with the structural water bridging the Thr98 carbonyl and Asp60 side chain, while the acetanilide methyl group forms van der Waals contacts with the 97-98 backbone. The P1′ sulfone isopropyl group forms a close contact with the Cys42Sγ (closest C – S contact = 3.8 Å). Importantly, the proximity of the acetanilide methyl and P2 phenyl groups suggested that these positions might be linked to generate macrocyclic inhibitors (Figure 1C), which we hoped would have increased potency and selectivity and would provide a novel template for optimization to an orally bioavailable inhibitor.

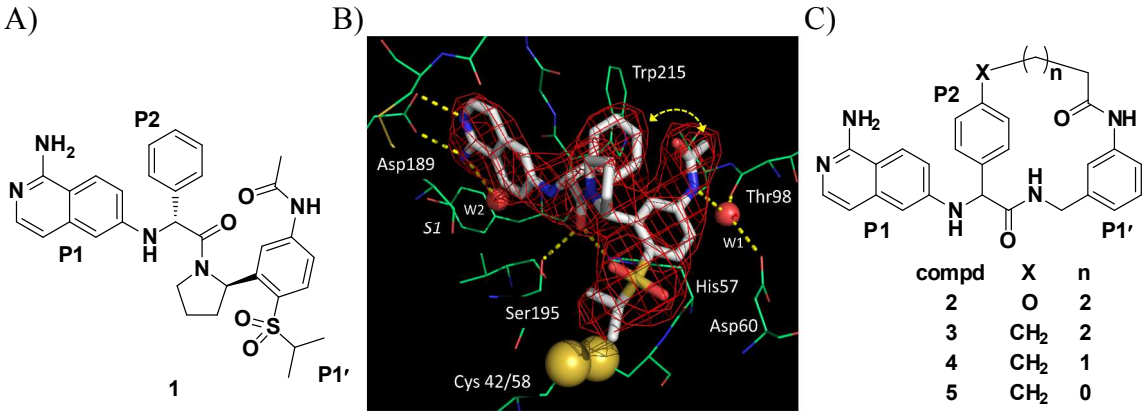

Figure 1. (A) Pyrrolidine phenylglycinamide lead **1**. **(**B) Crystal structure of **1** bound to FVIIa at 2.6 Å resolution.[58,59] The proximity of the P1′ acetanilide and P2 phenyl groups suggested that macrocyclization was feasible, as indicated by the double-headed yellow arrow. (C) Initial macrocycle synthetic targets.

A series of macrocyclic structures containing various linkers joining the *para* position of the P2 phenyl with the *meta* position of the P1′ phenyl were initially evaluated using a simulated annealing protocol implemented in the molecular dynamics software package Discover_3.[60] Structures which maintained key van der Waals and hydrogen bonding interactions were then subjected to conformational analysis to estimate the ligand strain induced by binding. In order to ensure an acceptable level of accuracy and reliability, we elected to assess the ligand strain energy using quantum chemical methods

(for details, see the Experimental section). Of the 15 linker structures evaluated, butanamide appeared most promising in that key intermolecular interactions were maintained while incurring little binding strain. Figure 2 shows that the calculated global quantum chemical energy minimum for a macrocycle containing the butanamide linker closely matches the crystallographically determined FVIIa bound conformation of **1**. Longer 4-oxybutanamide and pentanamide linkers, while also engaging in the key interactions, exhibited higher degrees of binding strain and greater flexibility, each possessing a relatively large number of lower energy conformations. Other linkers either did not maintain key intermolecular interactions or showed higher binding strain. Based on these results, we targeted the synthesis of macrocycles **2**-**4**, containing the 4-oxybutanamide, pentanamide, and butanamide linkers, respectively. We also targeted **5**, containing a shorter propionamide linker, in order to generate a homologous series of 15- to 17-membered macrocycles (Figure 1C). We retained the aminoisoquinoline group of **1** in our targeted compounds, as it is less basic than benzamidine[61] and offers better prospects for achieving oral bioavailability.

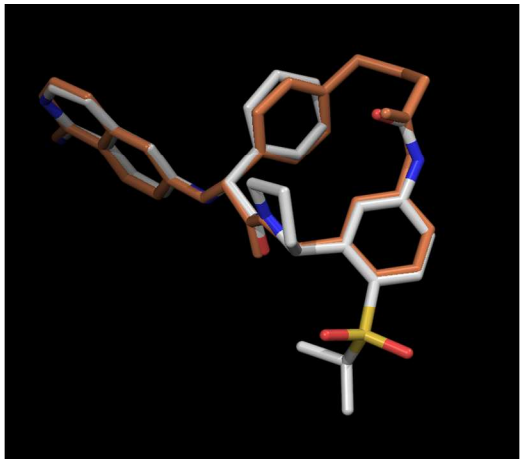

Figure 2. Overlay of the calculated global quantum chemical energy minimum of macrocycle **4** (orange)**,** containing the butanamide linker, on the crystal structure of **1** (white) bound to FVIIa.[59]

Chemistry

As shown in Scheme 1, the general synthetic route for preparing macrocycles **2-5** involves 3 key steps: 1) preparation of appropriately functionalized boronic acids, 2) Petasis reaction with a P1 aniline intermediate (**9**) and glyoxylic acid to form the phenylglycine core (**10**),[62] and 3) macrocyclization to form the upper amide bond. Specifically, for macrocycle **2**, 4-(4-bromophenylphenoxy)butyric acid **6a** was coupled with bis(neopentyl glycolato)diboron,[63] followed by hydrolysis to the free boronic acid **7a**. The carboxylate was alkylated with benzyl bromide to give ester **8a**. Petasis reaction of **8a** with bis-Boc protected 1-aminoisoquinoline intermediate **9**[26] and glyoxylic acid afforded the key phenylglycine intermediate **10a** in 68% yield. Subsequent amide coupling to *m*-nitrobenzylamine provided the fully protected macrocyclization precursor **11a**. Deprotection of the benzyl ester and reduction of the nitro group was accomplished by hydrogenation, followed by macrolactamization with EDC/HOAt and final Boc removal with hydrogen chloride, which gave macrocycle **2** in 25 % yield over three steps. In a similar fashion, commercially available acids **6b**, **6c**, and **7d** were elaborated to macrocycles **3**, **4**, and **5**, respectively. Macrocycle **4** was separated by chiral HPLC into its enantiomers **(*R*)-4** and **(*S*)-4**. Acyclic compounds **15** and **16** were prepared by Petasis reaction and amide formation as shown in Scheme 1.

Scheme 1. Synthesis of macrocycles **2-5**[a]

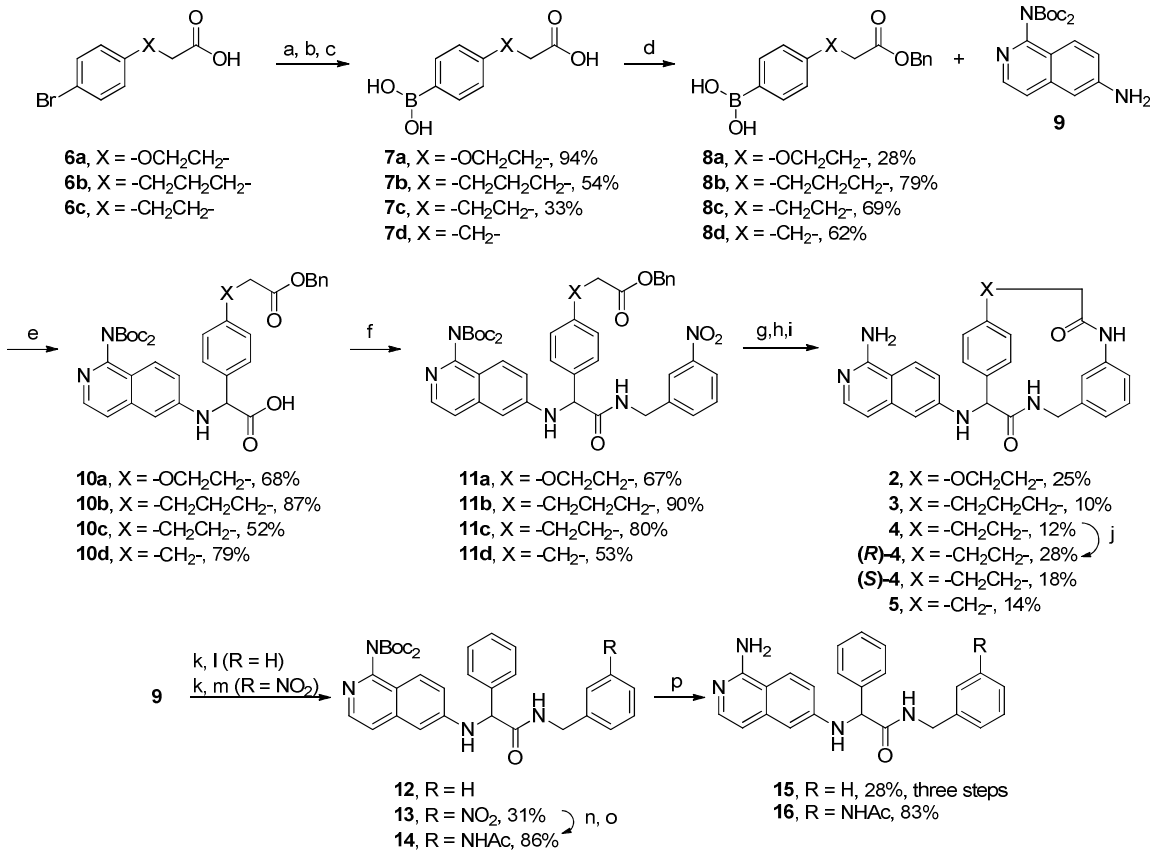

[a] (a) bis(neopentyl glycolato)diboron, $PdCl_2$(dppf), KOAc, DMSO, 80 °C; (b) 2M NaOH; (c) 6M $HCl_{(aq)}$; (d) benzyl bromide, $KHCO_3$, DMF, 60 °C; (e) glyoxylic acid monohydrate, 1,2-dichloroethane, 100 °C, μwave; (f) *m*-nitrobenzylamine·HCl, EDC, HOAt, DIEA, CH_2Cl_2, DMF; (g) H_2, 10% Pd/C, MeOH, (h) EDC, HOAt, DIEA, CH_2Cl_2, DMF; (i) 4N HCl/dioxane/EtOAc (**2**, **5**) or 50% TFA/CH_2Cl_2 (**3**, **4**); (j) chiral HPLC separation (Chiralcel OD, 30% (1:1 MeOH:EtOH)/heptane); (k) phenylboronic acid, glyoxylic acid monohydrate, acetonitrile, DMF, 100 °C, μwave; (l) benzylamine, BOP, DIEA; (m) *m*-nitrobenzylamine, BOP, DIEA; (n) Zn, NH_4Cl, MeOH, THF; (o) AcCl, DIEA, acetonitrile; (p) TFA, CH_2Cl_2.

Initial attempts to prepare sulfonyl-substituted macrocycles **23**-**25** and **31** (Scheme 2) via macrolactamization at the anilide bond were unsuccessful presumably due to the poor nucleophilicity of the electron-deficient *para*-sulfonylaniline. A modified route, in which the anilide bond was formed

early in the synthesis, followed by macrolactamization at the phenylglycine amide, successfully delivered the target compounds (Scheme 2). Beginning with 2-fluoro-5-nitrobenzonitrile **17**, substitution with ethanethiol followed by oxidation gave ethylsulfone **18a.** The nitro group of **18a** was reduced to give aniline **19a** by hydrogenation and then reacted with the acid chloride prepared from **6c** in the presence of DMAP to give anilide **20a**. Anilide **20a** was cross coupled with bis(neopentyl glycolato)diboron and the resulting boronic ester was isolated as the diethanolamine adduct,[64] and then hydrolyzed to boronic acid **21a** during purification. Petasis reaction of **21a** with aminoisoquinoline **9** and glyoxylic acid gave phenylglycine intermediate **22a**. The latent benzylamine in **22a** was revealed by hydrogenation of the nitrile. Subsequent BOP-mediated macrolactamization, Boc deprotection, and chiral HPLC separation provided ***(R)*-23** in 20% yield over 4 steps**. *(R)*-24** and ***(rac)*-25** were prepared in similar fashion from **17**. In the case of benzamidine macrocycle ***(R)*-31**, the nitrile group in precursor **18a** was reduced and Boc protected early in the synthesis to give benzylamine **26**, which was elaborated to boronic acid **28**. Petasis reaction of **28** with *p*-aminobenzonitrile and glyoxylic acid gave phenylglycine intermediate **29**. Subsequent Boc deprotection, BOP-mediated macrolactamization, and chiral separation afforded benzonitrile ***(R)*-30.** This benzonitrile was converted to the amidoxime by treatment with hydroxylamine, followed by acetylation and hydrogenation to provide benzamidine ***(R)*-31**.

Scheme 2. Synthesis of macrocycles **23-25** and **31**[a]

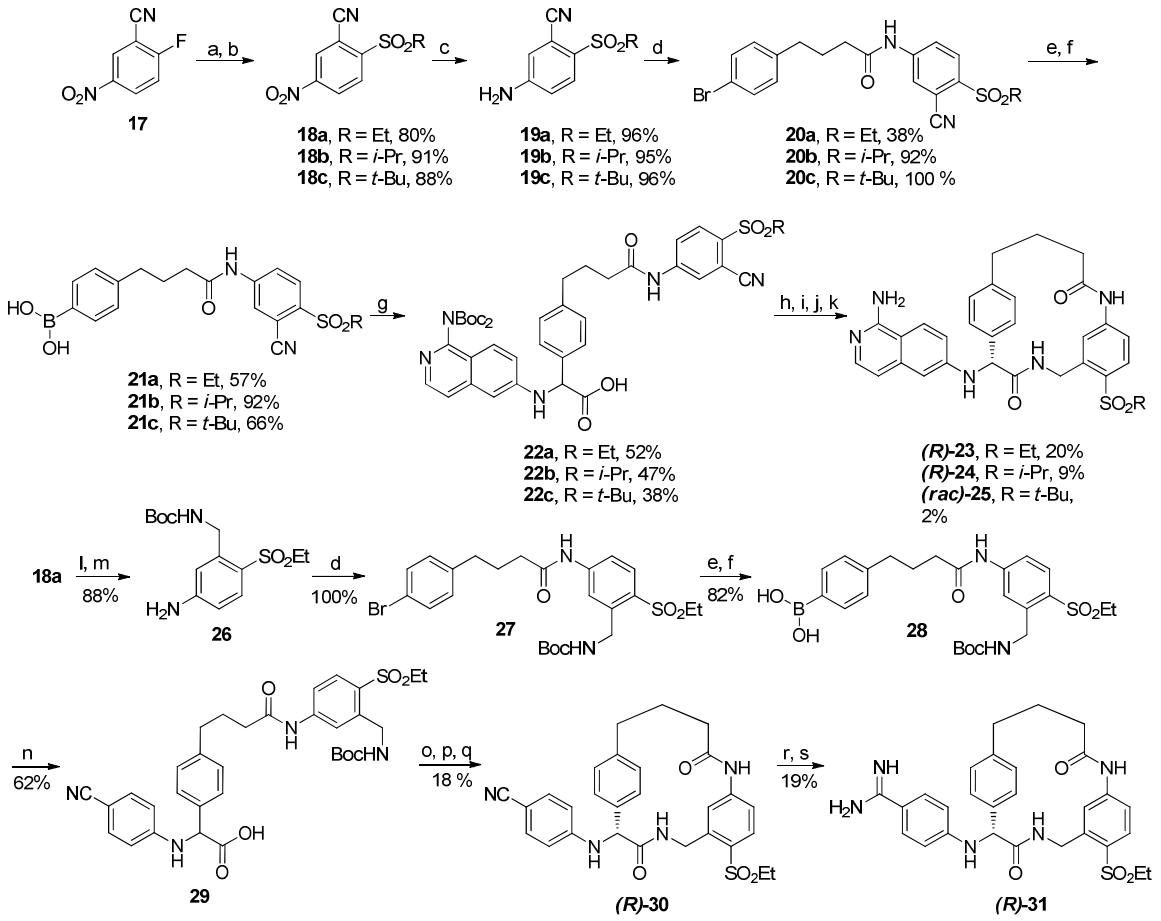

[a] (a) RSH, Et_3N, DMF; (b) *m*-CPBA, CH_2Cl_2; (c) H_2, 10% Pd/C, MeOH; (d) **6c**, $(COCl)_2$, DMF, CH_2Cl_2, then DMAP, Et_3N, 1,2-DCE, reflux; (e) bis(neopentyl glycolato)diboron, $PdCl_2$(dppf), KOAc, DMSO, 80 °C; (f) diethanolamine (g) **9**, glyoxylic acid monohydrate, DCE, μwave, 100 °C; (h) H_2, 10% Pd/C, 1M $HCl_{(aq)}$, MeOH; (i) BOP, DIEA, DMF; (j) 50% TFA, CH_2Cl_2; (k) chiral HPLC (Chiralcel OD-H, 30% (1:1 MeOH:EtOH) in heptane); (l) H_2, 10% Pd/C, 1M $HCl_{(aq)}$, MeOH, 9 days; (m) BOC-ON, Et_3N, THF; (n) *p*-aminobenzonitrile, glyoxylic acid monohydrate, CH_3CN, DMF, μwave, 100 °C; (o) 4N HCl/dioxane; (p) BOP, DMAP, CH_2Cl_2, DMF, 40 °C; (q) chiral HPLC (Chiralcel OD, 30% (1:1 MeOH:EtOH) in heptane); (r) NH_2OH, DMSO; (s) Ac_2O, CH_2Cl_2, then H_2, 10% Pd/C, MeOH.

Methylated macrocycle ***(R)*-37** was prepared as described in Scheme 3. Methyl but-3-enoate **32** was hydroborated with 9-BBN, coupled with 5-bromo-2-iodotoluene using $PdCl_2$(dppf),[65] and then

saponified to give carboxylate **33**. Subsequent amide formation with **19a** provided **34**, which was advanced to ***(R)*-37** using a sequence analogous to that which was used to prepare ***(R)*-23** from **20a**.

Scheme 3. Synthesis of macrocycle **37**[a]

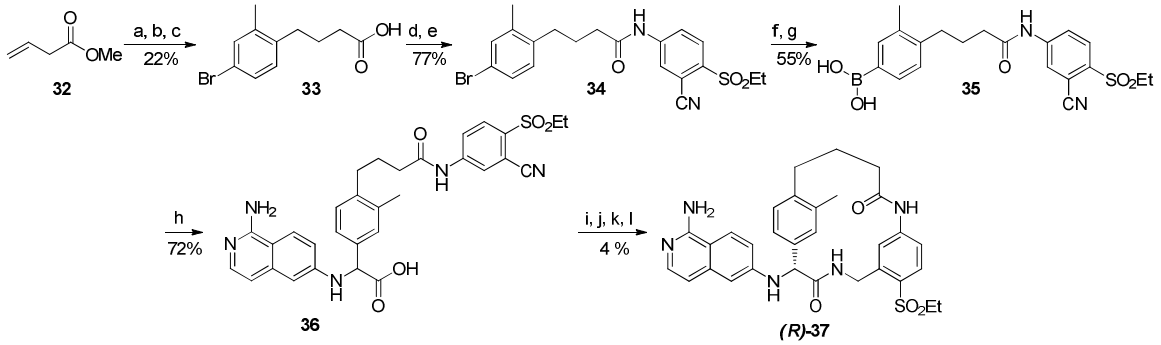

[a] (a) 9-BBN; (b) 5-bromo-2-iodotoluene, $PdCl_2$(dppf), NaOMe, THF, 70 °C; (c) NaOH, THF, MeOH, 80 °C; (d) $(COCl)_2$, DMF, CH_2Cl_2; (e) **19a**, toluene, reflux; (f) bis(neopentyl glycolato)diboron, $PdCl_2$(dppf), KOAc, DMSO, 80 °C; (g) $NaOH_{(aq)}$; (h) **9**, glyoxylic acid monohydrate, CH_3CN, DMF, μwave, 100 °C; (i) H_2, 10% Pd/C, 1M $HCl_{(aq)}$, MeOH; (j) BOP, DIEA, DMF; (k) 50% TFA, CH_2Cl_2; (l) chiral SFC (Chiralpak AS, 75% CO_2/25% MeOH/0.1% diethylamine, 100 bar, 40 °C).

Results and Discussion

Based on the results of the molecular modeling experiments, macrocycles **2-5** were prepared and assayed for inhibition of TF/FVIIa (Table I). Consistent with the predictions from the modeling data, the 16-membered macrocycle **4** was at least 5-fold more potent than either 17-membered macrocycles **2** and **3** or 15-membered macrocycle **5**. Comparison of macrocycle **4** with acyclic analog **15** indicated that incorporation of the optimized linker improved potency 60-fold. Comparison of **4** and **15** with acyclic compound **16** containing an acetamide group (representing the portion of the linker which interacts with S2) shows that the acetamide moiety contributes 5-fold to potency. Thus, the embedded amide is a key element of the macrocyclic linker of **4**, and the conformational constraint imposed by macrocyclization

presumably contributes an additional 11-fold potency increase relative to **16**. Racemic macrocycle **4** was separated into its enantiomers **(*R*)-4** and **(*S*)-4** by chiral HPLC, and all of the inhibitory activity was found to reside in the *R*-enantiomer (Table I, see below for stereochemical assignment).

Table I. Initial Linker Optimization of Phenylglycine Macrocycles

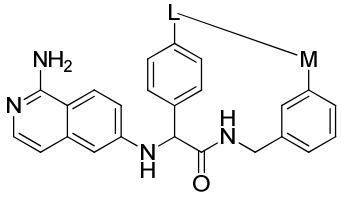

compd	L[a]	M	TF/FVIIa K_i (nM) [b]
2	$-OCH_2CH_2CH_2-$	-C(=O)NH-	4600
3	$-CH_2CH_2CH_2CH_2-$	-C(=O)NH-	6100
4	$-CH_2CH_2CH_2-$	-C(=O)NH-	920
(*R*)-4	$-CH_2CH_2CH_2-$	-C(=O)NH-	400
(*S*)-4	$-CH_2CH_2CH_2-$	-C(=O)NH-	>18000
5	$-CH_2CH_2-$	-C(=O)NH-	4600
15	H	H	54000
16	H	$CH_3C(=O)NH-$	10000

[a] atom connectivity is P2 phenyl-L-M-P1′ phenyl as the linker atoms are shown left to right. [b] TF/FVIIa K_i values were obtained from recombinant human enzyme and were averaged from two experiments.[12]

We crystallized FVIIa with racemic macrocycle **4** and determined the structure of the resulting complex at 2.06 Å resolution. In the crystal structure, the active site of FVIIa was occupied by the *R*-enantiomer of **4** (Figure 3A), consistent with the preferred stereochemistry previously observed for the pyrrolidine phenylglycinamide series.[26] The stereochemistry of the active enantiomer of **4** (Table I), and the other macrocycles containing this linker was therefore assigned as *R*. An overlay of **(*R*)-4** with phenylpyrrolidine **1** indicates that the five-atom butanamide linker provides an essentially optimal

geometric constraint (Figure 3B), in full agreement with the molecular modeling data (Figure 2). Macrocycle **(*R*)-4** thus engages in very similar intermolecular interactions as those described for **1** in Figure 1. Key interactions with Asp 189 in S1 are maintained and the linker anilide NH engages in a hydrogen bond with the aforementioned conserved water molecule in S2 (Figure 3A).

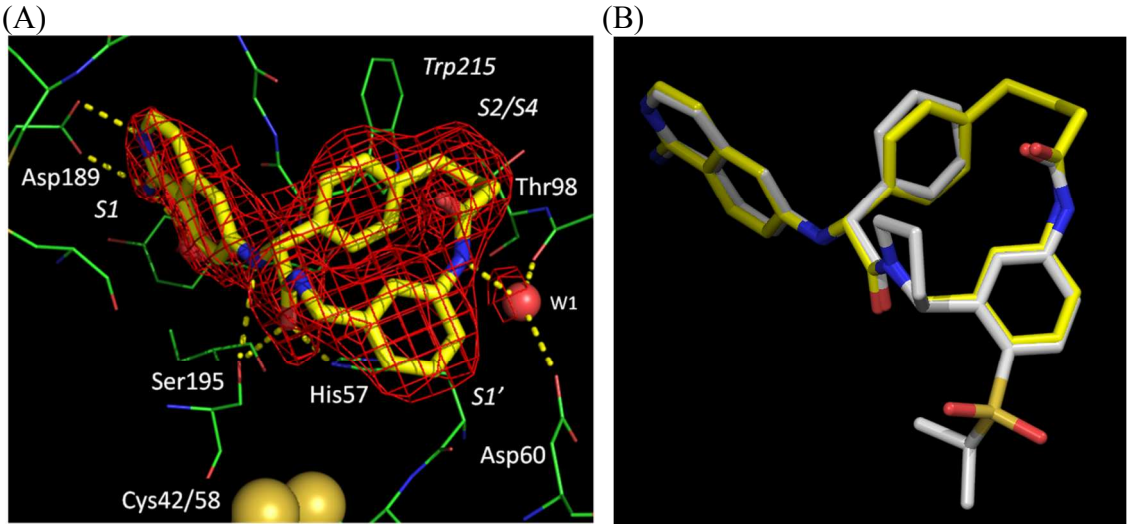

Figure 3. (A) Crystallographic structure of **(*R*)-4** in FVIIa at 2.06 Å resolution.[59,66] (B) Overlay of **1** and **(*R*)-4** bound to FVIIa.[67]

Based on structure activity relationships established in the phenylpyrrolidine series,[26] in which a P1′ alkyl sulfone can improve potency >20-fold relative to hydrogen, and the excellent structural overlay of **1** with **(*R*)-4** shown in Figure 3B, we incorporated a P1′ alkyl sulfone group to improve the potency of the macrocycles (Scheme 2). As shown in Table II, introduction of an ethylsulfone to give ***(R)*-23** improved TF/FVIIa potency 50-fold relative to **(*R*)-4** and improved activity in the FVII-deficient prothrombin time assay by 16-fold, demonstrating promising activity in plasma.[12] Additionally, ***(R)*-23** has significantly improved selectivity against a panel of seven related serine proteases, particularly vs. activated protein C (APC) and tissue kallikrein-1, with 160-fold and 12-fold selectivity, respectively. Isopropylsulfone ***(R)*-24** is slightly more potent than ***(R)*-23**, while tert-butyl sulfone ***(rac)*-25** is about 2-

fold less potent than ***(R)*-23**, considering that the former is racemic. Incorporation of a highly basic benzamidine P1 group afforded ***(R)*-31**, which has 11-fold improved potency relative to aminoisoquinoline ***(R)*-23**, but reduced selectivity (58- and 83-fold selectivity vs. APC and trypsin, respectively). Incorporation of a methyl group in ***(R)*-37** as described in Scheme 3, in order to fill the small, hydrophobic S2 pocket in FVIIa, improved potency 5-fold relative to ***(R)*-23**, and increased selectivity vs. the serine protease panel (APC and tissue kallikrein-1 selectivity for ***(R)*-37** is >500-fold and 62-fold, respectively). Importantly, ***(R)*-37** has 5-fold improved TF/FVIIa potency and 10-fold improved FVII-deficient prothrombin time EC_{2x} relative to the original phenylpyrrolidine lead, **1**. This high level of enzyme inhibitory potency and activity in plasma is promising for further optimization. It is also important to note that ***(R)*-37** exists as a 1:1 mixture of two conformational isomers at room temperature (likely atropisomers due to hindered rotation of the unsymmetrically substituted P2 phenyl group). Control of the conformational dynamics of this scaffold may enable additional potency and selectivity improvements.

Table II. Potent Macrocyclic Sulfones [a]

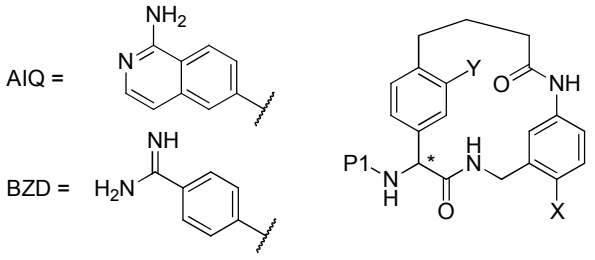

compd	P1	X	Y	TF/FVIIa K_i (nM)	FIXa K_i (nM)	FXa K_i (nM)	Thrombin K_i (nM)	APC K_i (nM)	Trypsin K_i (nM)	Plasma Kall. K_i (nM)	Tissue Kall. K_i (nM)	FVII def. [b] PT EC_{2x} (μM)
(*R*)-4	AIQ	H	H	400	>35000	>9000	>13000	2800	>6000	>6000	18	26
(*R*)-23	AIQ	$-SO_2Et$	H	8.0	>35000	3200	5800	1300	3600	4600	100	1.6
(*R*)-24	AIQ	$-SO_2$-*i*-Pr	H	5.2	>35000	3300	4000	1800	3000	3600	100	1.4

(*rac*)-25	AIQ	-SO_2-*t*-Bu	H	30	>35000	4800	>13000	14000	>6000	>6000	22	8.6
(*R*)-31	BZD	-SO_2Et	H	0.70	34000	5500	180	41	58	50	1900	0.42
(*R*)-37	AIQ	-SO_2Et	Me	1.6	16000	1000	6700	830	2700	1700	100	1.2

[a] K_i values were averaged from two experiments. TF/FVIIa assays were performed with recombinant human enzyme, while other enzyme assays were performed with purified human enzymes. All assays were run at room temperature (25 °C), except tissue kallikrein-1, which was run at 37 °C. See reference 12 for a detailed description of the enzyme assay protocols. APC = activated protein C. Tissue Kall. = tissue kallikrein-1. [b] see reference 12 for a detailed description of the FVII-deficient prothrombin time assay.

Conclusions

Based on a crystal structure of phenylpyrrolidine lead **1** and subsequent molecular modeling, we designed a novel series of macrocyclic FVIIa inhibitors. The optimal 16-membered macrocycle **4** was 60-fold more potent than the corresponding acyclic analog **15**. Further potency optimization by incorporation of P1′ ethyl sulfone and P2 methyl substituents provided ***(R)*-37**, with TF/FVIIa K_i = 1.6 nM, excellent selectivity against a panel of seven serine proteases, and FVII-deficient prothrombin time EC_{2x} = 1.2 μM. The macrocyclic FVIIa inhibitor chemotype exemplified by ***(R)*-37** provides a novel, potent, and selective scaffold for further optimization towards an orally bioavailable drug candidate. The results of our efforts to achieve this goal will be reported in due course.

Experimental Section

Crystallization, data collection and structure refinement. Recombinant full-length FVIIa was purchased from Novo Nordisk. The GLA domain (residues 1–44) was removed by Cathepsin G digestion. The final protein concentration was approximately 25 mg/ml. Single crystals suitable for x-ray analysis were obtained by vapor diffusion. The crystals were grown at 4° C with 20% PEG 6000, 20 mM $CaCl_2$, 0.1M MES (pH 6.0) in the reservoir.

Data for the FVIIa crystals in complex with ligands were collected at 17-ID [IMCA Collaborative Access Team (IMCA-CAT)] located at the Advanced Photon Source (APS) or in the laboratory with a

Rigaku FR-E superbright generator, Rigaku MicroMax® confocal optics, and a Rigaku Saturn 92 detector.

Image data were processed with the program HKL.[68] The CNX program (Accelrys) was used for crystallographic refinement.[69] The atomic coordinates of human FVIIa (1DAN)[2] were used as a search model. Molecular replacement and rigid body refinement were performed with 8.0 to 3.5 Å resolution data. The FVIIa coordinates were subjected to a few cycles of atomic positional refinements. Simulated annealing (at a maximum temperature of 3000 K) was followed by B-factor refinement. Examination of the resulting Fo-Fc electron density map revealed the density for the compound and allowed unambiguous fitting of the compound. The inhibitors were built with the program QUANTA (Accelrys). Peaks in the difference electron density map which were greater than 3σ and which were less than 3.5 Å away from the protein were built in as solvent molecules. No major adjustments to the protein model were needed during the course of the refinements. The structure was re-refined prior to deposition using BUSTER (GlobalPhasing, Ltd), GRADE (GlobalPhasing, Ltd), for the ligand restraint files, RHOFIT (GlobalPhasing, Ltd), for ligand placement and COOT[70] for electron density map fitting. Coordinates and structure amplitudes have been deposited in the PDB with accession codes of 4ZXX and 4ZXY**.**

Molecular Modeling. Idea structures were initially evaluated using a simulated annealing protocol implemented in the Discover_3 molecular dynamics package[60] and utilizing the CFF98 forcefield.[71-75] Typically, a model of the idea structure bound in FVIIa was subjected to molecular dynamics at 310 K (gas phase with a distance dependent dielectric), while allowing several contact amino acids and side chains in the active site to relax. Snapshots were taken at 10 picosecond intervals, and then minimized. Idea structures which maintained key van der Waals and hydrogen bonding interactions were then subjected to an extended conformational analysis to assess the ligand strain requirement upon binding. Initial conformation generation was performed using the mixed Monte Carlo-low mode search algorithm

in the MacroModel software package using the OPLS-AA-2001 forcefield with the GBSA solvation model.[76] To avoid unrealistic intramolecular electrostatic interactions, the amidine was neutralized in this and subsequent steps in the conformational analysis. Conformations within 5 kcal of the observed global minimum[77, 78] were further minimized with the quantum chemistry software package Jaguar using B3LYP/6-31G**.[79] Final single point energies were computed using the local MP2 method implemented in Jaguar with the pseudospectral cc-pVTZ(-f)++ basis set. In general, the observed global minimum was taken as the lowest energy structure. Strain of the bound conformation was estimated in two ways. **Method 1**: The annealed idea structure was removed from the protein and the equilibrium structure was obtained at B3LYP/ 6-31G** in which only angles and bonds were allowed to equilibrate. The strain was assessed by comparing the LMP2-/ cc-PVTZ energies of this partially relaxed pose and the observed global minimum. **Method 2**: Identical to Method 1 except the idea structure was allowed to fully relax to its nearest local minimum. We sometimes observed that although this structure was conformationally similar to the one obtained in Method 1, it was significantly lower in energy and so provided a better measure of strain. See Supporting Information Figure S1 for a summary of the linkers evaluated.

Biological Assays. The TF/FVIIa, FIXa, FXa, thrombin, activated protein C, trypsin, plasma kallikrein, and tissue kallikrein-1 enzyme assays and the FVII-deficient prothrombin time assay were performed according to published protocols.[12]

General Chemistry Methods. All reactions were carried out using commercial grade reagents and solvents. Solution ratios express a volume relationship, unless stated otherwise. NMR chemical shifts (δ) are reported in parts per million relative to internal TMS. Flash chromatography was carried out on ISCO CombiFlash™ systems using prepacked silica cartridges and eluted with gradients of the specified solvents. Preparative reverse phase high pressure liquid chromatography (HPLC) was carried out on C_{18} HPLC columns using methanol/water gradients containing 0.1% trifluoroacetic acid. Purity of all final

compounds was determined to be ≥ 95% by analytical HPLC using the following conditions: Phenomenex Luna C18 column (4.6 x 75 mm) eluted at 4 mL/min with an 8 min gradient from 100% solvent A to 100% solvent B (solvent A: 10% methanol, 89.9% water, 0.1% H_3PO_4; solvent B: 90% methanol, 9.9% water, 0.1% H_3PO_4), monitoring uv absorbance at 220 nM.

4-(4-Boronophenoxy)-butyric acid (7a). A resealable tube was charged with 4-(4-bromophenoxy)butyric acid **6a**, (259 mg, 1.0 mmol), bis(neopentyl glycolato)diboron (249 mg, 1.1 mmol), potassium acetate (245 mg, 2.5 mmol), and DMSO (2 mL). The resulting orange suspension was deoxygenated by sparging with nitrogen gas. Dichloro[1,1'-bis(diphenylphosphino)ferrocene] palladium(II) dichloromethane adduct (30 mg, 0.041 mmol) was added, and the tube was sealed tightly and heated at 80°C overnight. Hydrochloric acid (1N) was added, and the mixture was extracted with EtOAc (2x), washed with water (2x) and brine (1x), and dried ($MgSO_4$). The organic layer was concentrated *in vacuo* and the residue purified by flash chromatography (0 to 15% MeOH in DCM) to give the 2,2-dimethyl-1,3-propanediol boronic ester of **7a**. This material was dissolved in diethyl ether and washed with NaOH (2 N, 2x). The aqueous layers were washed with diethyl ether, combined, and acidified to pH 4 with hydrochloric acid (6 N). The resulting solid precipitate was collected by filtration to afford **7a** (210 mg, 94%) as a beige solid. ^{1}H NMR (400 MHz, CD_3OD) δ 2.06 (m, 2H), 2.48 (t, J = 7.5 Hz, 2H), 4.02 (t, J = 6.6 Hz, 2H), 6.88 (br s, 2H), 7.62 (br d, 2H).

4-(3-Benzyloxycarbonyl-propoxy)-phenylboronic acid (8a). A solution of **7a** (200 mg, 0.89 mmol), potassium bicarbonate (313 mg, 3.1 mmol), and benzyl bromide (0.163 mL, 1.4 mmol) in DMF (2 mL) was heated at 60°C for 8 h. The reaction mixture was concentrated *in vacuo* and the residue was partitioned between EtOAc and hydrochloric acid (1 N). The aqueous layer was extracted with EtOAc (2x) and then the combined organics were washed with water (3x) and brine, dried ($MgSO_4$), and concentrated *in vacuo*. The residue was purified by flash chromatography (30 to 100% EtOAc in

hexane) to afford **8a** (86 mg, 28%) as a white solid. ^{1}H NMR (400 MHz, CD_3OD) δ 2.08 (m, 2H), 2.56 (t, *J* = 7.0 Hz, 2H), 4.00 (m, 2H), 5.12 (s, 2H), 6.84 (2 x d, 2H), 7.32 (m, 5H), 7.7-7.5 (2 x d, 2H).

4-{4-[(1-Di-*tert*-butoxycarbonylamino-isoquinolin-6-ylamino)-carboxy-methyl]-phenoxy}-butyric acid benzyl ester (10a). A solution of **8a** (82 mg, 0.26 mmol), **9** (72 mg, 0.20 mmol),[26] and glyoxylic acid monohydrate (22 mg, 0.24 mmol) in DCE (1 mL) was heated at 100°C for 10 min in a microwave reactor. This solution was purified by flash chromatography (0 to 15% MeOH in DCM) to give **10a** contaminated with **8a** (110 mg, 2.5:1 **10a**/**8a**, 68% yield based on content of **10a**) as a yellow oil. MS (ESI) *m/z* 686.3 $(M+H)^+$. ^{1}H NMR (400MHz, CD_3OD) δ 1.21-1.30 (m, 18H), 1.97-2.10 (m, 2H), 2.46-2.55 (m, 2H), 3.88-4.02 (m, 2H), 5.09 (s, 2H), 5.17 (s, 1H), 6.68 (d, *J* = 1.8 Hz, 1H), 6.85 (d, *J* = 8.3 Hz, 2H), 7.21-7.34 (m, 7H), 7.41 (d, *J* = 6.2 Hz, 1H), 7.46 (d, *J* = 8.8 Hz, 2H), 7.63 (d, *J* = 9.2 Hz, 1H), 8.01 (d, *J* = 5.7 Hz, 1H).

4-{4-[(1-Di-*tert*-butoxycarbonylamino-isoquinolin-6-ylamino)-(3-nitro-benzylcarbamoyl)-methyl]-phenoxy}3-butyric acid benzyl ester (11a). A solution of **10a** (110 mg, 0.16 mmol), 3-nitrobenzylamine hydrochloride (36 mg, 0.19 mmol), DIEA (0.084 mL, 0.48 mmol), HOAt (22 mg, 0.16 mmol), and EDC (62 mg, 0.32 mmol) in a mixture of DCM (2 mL) and DMF (0.5 mL) was stirred at rt overnight. The reaction mixture was concentrated *in vacuo* and the residue was triturated with water and then purified by flash chromatography (0 to 10% MeOH in DCM) to give **11a** (88 mg, 67%). MS (ESI) *m/z* 820.3 $(M+H)^+$. ^{1}H NMR (400MHz, CD_3OD) δ 1.21-1.30 (m, 18H), 1.23-1.24 (m, 1H), 2.08 (quin, *J* = 6.6 Hz, 2H), 2.56 (t, *J* = 7.3 Hz, 2H), 4.00 (t, *J* = 5.9 Hz, 2H), 4.37-4.61 (m, 1H), 5.01-5.18 (m, 3H), 6.69 (s, 1H), 6.91 (d, *J* = 8.8 Hz, 2H), 7.25-7.35 (m, 7H), 7.39 (d, *J* = 6.6 Hz, 2H), 7.46 (d, *J* = 8.3 Hz, 2H), 7.50-7.58 (m, 1H), 7.61-7.70 (m, 1H), 7.97 (s, 1H), 7.99-8.03 (m, 2H), 8.06 (d, *J* = 6.2 Hz, 1H).

2-(1-Amino-isoquinolin-6-ylamino)-16-oxa-4,11-diaza-tricyclo[15.2.2.1^{6,10}]docosa-1(20),6,8,10(22),17(21),18-hexaene-3,12-dione trifluoroacetic acid salt (2). A solution of **11a** (88 mg, 0.11 mmol) in MeOH was hydrogenated (55 psi) over 10% palladium on carbon (36 mg) for 3 h. The

reaction mixture was filtered and concentrated *in vacuo* to give a yellow glass (73 mg). A portion of this material (63 mg) in a mixture of DCM (10 mL) and DMF (0.5 mL) was treated with DIEA (0.047 mL, 0.27 mmol), HOAt (12 mg, 0.088 mmol), and EDC (35 mg, 0.18 mmol) and the mixture was stirred at rt overnight. The reaction mixture was concentrated *in vacuo*. A solution of the residue combined with the product from 2 mg and 4 mg scale pilot reactions in EtOAc (0.5 mL) and hydrogen chloride in dioxane (1 mL, 4N) was stirred at rt for 3 h. The reaction mixture was concentrated *in vacuo* and the residue was purified by reverse phase HPLC to give **2** (15 mg, 25%) as a white solid. MS (ESI) *m/z* 482.3 $(M+H)^+$. ^{1}H NMR (400 MHz, CD_3OD) δ 2.03 - 2.19 (m, 2H), 2.44 - 2.58 (m, 2H), 3.95 (dd, *J* = 15.38, 3.52 Hz, 1H), 4.03-4.19 (m, 2H), 4.73 (dd, *J* = 15.38, 8.35 Hz, 1H), 5.09 (s, 1H), 5.50 (s, 1H), 6.70 (s, 1H), 6.82 (d, *J* = 7.03 Hz, 1H), 6.93 (d, *J* = 8.35 Hz, 3H), 7.10 - 7.20 (m, 3H), 7.29 (d, *J* = 7.03 Hz, 1H), 7.46 (d, *J* = 7.03 Hz, 2H), 7.52 (d, *J* = 7.47 Hz, 1H), 8.05 (d, *J* = 9.23 Hz, 1H), 8.49 (dd, *J* = 7.91, 3.95 Hz, 1H).

2-(Ethylsulfonyl)-5-nitrobenzonitrile (18a). Ethanethiol (2.8 mL, 38 mmol) was added to a solution of 2-fluoro-5-nitrobenzonitrile **17** (5.00 g, 30.1 mmol) and triethylamine (9.3 mL, 67 mmol) in DMF (100 mL). The reaction mixture was stirred for 1 h and then poured into water (500 mL). The resulting precipitate was isolated by filtration, dissolved in DCM, washed with water and brine, dried ($MgSO_4$), and concentrated under reduced pressure. The residue (6.14 g) was dissolved in DCM (100 mL), cooled to 0°C, and treated with *m*-CPBA (16.0 g, 71 mmol) in one portion. The reaction mixture was allowed to stir at rt overnight, and then was extracted with sodium bicarbonate solution (saturated), sodium bisulfite solution (10%), and brine. The organic layer was dried ($MgSO_4$) and concentrated under reduced pressure to afford **18a** (5.6 g, 80%) as a pale yellow solid. ^{1}H NMR (400 MHz, $CDCl_3$) δ 1.02 (s, 6H), 1.97 (m, 2H), 2.36 (t, *J* = 7.5 Hz, 2H), 2.68 (t, *J* = 7.7 Hz, 2H), 3.76 (s, 4H), 7.18 (d, *J* = 7.9 Hz, 2H), 7.72 (d, *J* = 7.5 Hz, 2H).

5-Amino-2-(ethylsulfonyl)benzonitrile (19a). A solution of **18a** (0.554 g, 2.31 mmol) in MeOH (60 mL) was hydrogenated (60 psi) over 10% palladium on carbon (99 mg) for 3 h at rt. The reaction

mixture was filtered and concentrated under reduced pressure to give **19a** (464 mg, 96%) as an off-white solid. ^{1}H NMR (400 MHz, $CDCl_3$) δ 1.30 (t, *J* = 7.25 Hz, 3H), 3.30 (q, *J* = 7.47 Hz, 2H), 4.62 (s, 2H), 6.89 (dd, *J* = 8.79, 2.64 Hz, 1H), 7.04 (d, *J* = 2.20 Hz, 1H), 7.83 (d, *J* = 8.79 Hz, 1H).

4-(4-Bromophenyl)-N-(3-cyano-4-(ethylsulfonyl)phenyl)butanamide (20a). Oxalyl chloride (0.175 mL, 2.0 mmol) was added slowly dropwise to a solution of 4-(4-bromophenyl)butyric acid (243 mg, 1.0 mmol) in DCM (3 mL) and DMF (2 drops). The reaction was stirred for 1 h at rt and then concentrated under reduced pressure. The residue was coevaporated with toluene and then chloroform to give the acid chloride as a crude brown oil. A solution of the crude acid chloride (197 mg, 0.75 mmol) and **19a** (106 mg, 0.50 mmol) in DCM (1 mL) was treated with triethylamine (0.140 mL, 1.0 mmol) and DMAP (10 mg, 0.08 mmol). The reaction mixture was stirred for 14 h at rt. DCE (1 mL) was added, and the reaction mixture was heated to reflux for 30 h. The reaction was cooled to rt, diluted with DCM, and washed with 1 N HCl, dried ($MgSO_4$), and concentrated under reduced pressure. The residue was purified by silica gel chromatography (EtOAc/hexanes) and then by reverse phase HPLC to give **20a** (83 mg, 38%). MS (ESI) *m/z* 435.2, 437.2 $(M+H)^+$. ^{1}H NMR (400MHz, $CDCl_3$) δ 1.32 (t, *J* = 7.5 Hz, 3H), 2.06 (quin, *J* = 7.4 Hz, 2H), 2.42 (t, *J* = 7.3 Hz, 2H), 2.68 (t, *J* = 7.5 Hz, 2H), 3.35 (q, *J* = 7.5 Hz, 2H), 7.08 (d, *J* = 7.9 Hz, 2H), 7.41 (d, *J* = 8.3 Hz, 2H), 7.67 (s, 1H), 7.88 (dd, *J* = 8.8, 1.8 Hz, 1H), 8.04 (d, *J* = 8.8 Hz, 1H), 8.16 (d, *J* = 2.2 Hz, 1H).

4-(4-(3-Cyano-4-(ethylsulfonyl)phenylamino)-4-oxobutyl)phenylboronic acid (21a). A flask containing **20a** (83 mg, 0.19 mmol), bis(neopentyl glycolato)diboron (47.6 mg, 0.211 mmol), potassium acetate (83 mg, 0.84 mmol), and dichloro[1,1'-bis(diphenylphosphino)ferrocene] palladium(II) dichloromethane adduct (4.4 mg, 0.0060 mmol) was purged with argon. DMSO (1 mL) was added, and the reaction mixture was degassed with three cycles of vacuum followed by argon backfill. The reaction mixture was heated for 2 h at 80 °C, cooled to rt, and diluted with water (100 mL). The aqueous solution was extracted with diethyl ether (3x 25 mL), and the organic layers were dried ($MgSO_4$), and

concentrated under reduced pressure. The residue was dissolved in a mixture of diethyl ether (1 mL), DCM (~0.1 mL), and EtOAc (~0.1 mL). Diethanolamine (22 mg, 0.21 mmol) in isopropanol (0.5 mL) was added, and the reaction mixture was stirred overnight at rt. The reaction mixture was concentrated, and the residue was purified by reverse phase HPLC (under the standard acidic conditions) to give **21a** (44 mg, 57%) as a clear oil. MS (ESI) *m/z* 425.4 $(M+CH_3OH-H_2O+H)^+$. ^{1}H NMR (400MHz, tetrahydrofuran-d_8) δ 1.12-1.26 (m, 3H), 2.01 (quin, *J* = 7.3 Hz, 2H), 2.27-2.37 (m, 2H), 2.69 (t, *J* = 7.5 Hz, 2H), 3.24-3.39 (m, 2H), 3.74 (s, 3H), 7.09-7.19 (m, 2H), 7.67 (d, *J* = 7.5 Hz, 1H), 7.86-8.06 (m, 2H), 8.18-8.39 (m, 1H), 9.57-9.70 (m, 1H).

2-(1-Di-*tert*-butoxycarbonylaminoisoquinolin-6-ylamino)-2-(4-(4-(3-cyano-4-(ethylsulfonyl)phenylamino)-4-oxobutyl)phenyl)acetic acid (22a). Using a procedure analogous to that which was used to prepare **10a**, **21a** (43.6 mg, 0.109 mmol) was reacted with **9** and glyoxylic acid monohydrate to afford **22a** (42.8 mg, 52%) as a yellow solid. MS (ESI) *m/z* 772.3 $(M+H)^+$. ^{1}H NMR (400MHz, DMSO-d_6) δ 1.14 (t, *J* = 7.3 Hz, 3H), 1.31 (s, 18H), 1.85-1.97 (m, 2H), 2.41 (t, *J* = 7.5 Hz, 2H), 2.63 (t, *J* = 7.5 Hz, 2H), 3.39 (q, *J* = 7.5 Hz, 2H), 5.26 (s, 1H), 6.72 (s, 1H), 7.25 (d, *J* = 7.9 Hz, 2H), 7.33-7.43 (m, 2H), 7.46-7.54 (m, 3H), 8.02 (s, 2H), 8.07 (d, *J* = 5.7 Hz, 1H), 8.33 (s, 1H).

(*R*)-2-(1-Amino-isoquinolin-6-ylamino)-7-ethanesulfonyl-4,11-diaza-tricyclo[14.2.2.1^{6,10}]henicosa-1(19),6,8,10(21),16(20),17-hexaene-3,12-dione (*(R)*-23). A solution of **22a** (17 mg, 0.022 mmol) in a mixture of methanol (5 mL) and 1M hydrochloric acid (0.050 mL) was hydrogenated (60 psi) over 10% palladium on carbon (7 mg) for 17 h. The reaction mixture was filtered and concentrated under reduced pressure. A solution of the residue, DIEA (0.010 mL, 0.057 mmol), and BOP (5.3 mg, 0.012 mmol) in DMF (1.0 mL) was stirred at rt for 1 h. The reaction mixture was concentrated *in vacuo* and purified by reverse phase HPLC. The residue was dissolved in 50% TFA/DCM (1.5 mL) with 2 drops of water added and stirred for 1.25 h at rt. The solvent was evaporated under a stream of nitrogen and the residue was purified by reverse phase HPLC and then by chiral

HPLC to give ***(S)*-23** (peak 1, 2.6 mg, 21%) and ***(R)*-23** (peak 2, 2.4 mg, 20%). The chromatography conditions were the following: Chiralcel OD-H column (2.5 cm ID x 25 cm L, Chiral Technologies, Inc.), 30% (1:1 ethanol/methanol)/70% heptane as eluent, 15 mL/min flow rate, and uv detection at 254 nm. ***(R)*-23** analytical data: MS (ESI) *m/z* 558.3 $(M+H)^+$. ^{1}H NMR (400 MHz, CD_3OD) δ 1.24 (t, *J* = 7.51 Hz, 3H), 2.02-2.16 (m, 1H), 2.27-2.48 (m, 3H), 2.55-2.69 (m, 1H), 2.87-3.00 (m, 1H), 3.32-3.47 (m, 2H), 4.21 (d, *J* = 16.84 Hz, 1H), 5.05 (d, *J* = 16.84 Hz, 1H), 5.11 (s, 1H), 6.58 (d, *J* = 2.20 Hz, 1H), 6.64 (d, *J* = 1.46 Hz, 1H), 6.71 (d, *J* = 6.22 Hz, 1H), 6.91 (dd, *J* = 8.42, 2.20 Hz, 1H), 7.01 (dd, *J* = 8.97, 2.38 Hz, 1H), 7.05-7.16 (m, 2H), 7.40 (d, *J* = 7.69 Hz, 1H), 7.48 (d, *J* = 5.86 Hz, 1H), 7.59 (dd, *J* = 7.87, 1.65 Hz, 1H), 7.77 (d, *J* = 8.42 Hz, 1H), 7.83 (d, *J* = 9.15 Hz, 1H). Chiral analytical HPLC retention times: peak 1, 8.65 min; peak 2, 10.08 min using the following chromatography conditions: Chiralcel OD column (4.6 mm ID x 250 mm L, Chiral Technologies, Inc.), 30% (1:1 ethanol/methanol)/70% heptane as eluent, 1 mL/min flow rate, and uv detection at 254 nm.

***tert*-Butyl 5-amino-2-(ethylsulfonyl)benzylcarbamate (26).** A solution of **18a** (2.0 g, 8.32 mmol) in MeOH (100 mL) and hydrochloric acid (1 N, 20 mL) was hydrogenated (60 psi) over 20% $Pd(OH)_2$ (380 mg) for three days. The reaction mixture was filtered and hydrogenated twice more for three days each time over fresh catalyst. The reaction mixture was filtered and then concentrated *in vacuo* to give a white solid (2.15 g) after trituration with ethyl acetate and ether. 1.0 g of the solid was dissolved in THF (25 mL) and triethylamine (1 mL) and treated with 2-(*tert*-butoxycarbonyloxyimino)-2-phenylacetonitrile (0.905 g, 3.67 mmol). The reaction mixture was stirred overnight at rt. The reaction mixture was concentrated *in vacuo* and the residue was extracted twice with DCM and saturated sodium bicarbonate. The combined organics were extracted with brine, dried, and concentrated *in vacuo*. The residue was purified by silica gel chromatography (gradient from 0 to 50% ethyl acetate in hexanes) to give **26** (1.07 g, 88%) as a clear oil. MS (ESI) *m/z* 315.12 $(M+H)^+$. ^{1}H NMR (400MHz, $CDCl_3$) δ 1.21-

1.31 (m, 3H), 3.11 (q, *J* = 7.5 Hz, 2H), 4.43 (d, *J* = 6.6 Hz, 2H), 5.55 (br. s., 1H), 6.62 (dd, *J* = 8.6, 2.4 Hz, 1H), 6.81 (s, 1H), 7.70 (d, *J* = 8.8 Hz, 1H).

***tert*-Butyl 5-(4-(4-bromophenyl)butanamido)-2-(ethylsulfonyl)benzylcarbamate (27).** Using a procedure analogous to that which was used to prepare **20a**, except that pyridine was used in place of triethylamine, **26** (0.314 g, 1.00 mmol) was coupled to 4-(4-bromophenyl)butyric acid to give **27** (0.540 g, 100%) as a white foam. ^{1}H NMR (400 MHz, $CDCl_3$) δ ppm 1.23-1.31 (m, 3H) 1.41 (s, 9H) 1.97-2.08 (m, 2H) 2.37 (t, *J* = 7.47 Hz, 2H) 2.59-2.70 (m, 2H) 3.11-3.23 (m, 2H) 4.12 (q, *J* = 7.03 Hz, 1H) 4.50 (d, *J* = 6.15 Hz, 2H) 5.60 (t, *J* = 5.93 Hz, 1H) 7.06 (d, *J* = 8.35 Hz, 2H) 7.39 (d, *J* = 8.35 Hz, 2H) 7.45-7.50 (m, 1H) 7.83-7.95 (m, 2H).

4-(4-(3-((*tert*-Butoxycarbonylamino)methyl)-4-(ethylsulfonyl)phenylamino)-4-oxobutyl)phenylboronic acid (28). Using a procedure analogous to that which was used to prepare **21a**, **27** (0.541 g, 1.0 mmol) was coupled to bis(neopentyl glycolato)diboron (0.249 g, 1.1 mmol) and then hydrolyzed to the free boronic acid to give **28** (334 mg, 82%) as a peach colored foam. MS (ESI) *m/z* 505.03 $(M+H)^+$. ^{1}H NMR (400MHz, tetrahydrofuran-d_8) δ 1.17 (t, *J* = 7.3 Hz, 3H), 1.41 (s, 9H), 2.00 (t, *J* = 7.5 Hz, 2H), 2.27-2.35 (m, 2H), 2.68 (t, *J* = 7.3 Hz, 2H), 3.20 (q, *J* = 7.3 Hz, 2H), 4.53 (d, *J* = 6.2 Hz, 2H), 6.56 (br. s., 1H), 7.05 (s, 1H), 7.16 (d, *J* = 7.9 Hz, 2H), 7.63 (s, 1H), 7.70 (d, *J* = 7.9 Hz, 1H), 7.78-7.83 (m, 1H), 7.93 (d, *J* = 9.2 Hz, 1H).

2-(4-(4-(3-((*tert*-Butoxycarbonylamino)methyl)-4-(ethylsulfonyl)phenylamino)-4-oxobutyl)phenyl)-2-(4-cyanophenylamino)acetic acid (29). Using a procedure analogous to that which was used to prepare **10a**, **28** (0.101 g, 0.20 mmol) was reacted with 4-aminobenzonitrile (0.024 g, 0.2 mmol) and glyoxylic acid monohydrate (0.018 g, 0.2 mmol) to give, after purification by reverse phase HPLC, **29** (78 mg, 62%) as a white solid. MS (ESI) *m/z* 634.9 $(M+H)^+$. ^{1}H NMR (400MHz, CD_3OD) δ 1.11-1.27 (m, 3H), 1.44 (s, 9H), 1.92-2.04 (m, 2H), 2.40 (t, *J* = 7.3 Hz, 2H), 2.66 (t, *J* = 7.5 Hz, 2H),

3.20-3.31 (m, 2H), 4.57 (s, 2H), 6.66 (d, *J* = 9.2 Hz, 2H), 7.20 (d, *J* = 7.9 Hz, 2H), 7.35 (d, *J* = 9.2 Hz, 2H), 7.42 (d, *J* = 7.9 Hz, 2H), 7.75 (dd, *J* = 8.8, 2.2 Hz, 1H), 7.80-7.87 (m, 2H).

4-((*R*)-7-Ethanesulfonyl-3,12-dioxo-4,11-diaza-tricyclo[14.2.2.1^{6,10}]henicosa-1(19),6,8,10(21),16(20),17-hexaen-2-ylamino)-benzonitrile (*(R)*-30). Hydrogen chloride (4N solution in dioxane, 1 mL, 4 mmol) was added to a solution of **29** (78 mg, 0.12 mmol) in ethyl acetate (1 mL). The reaction mixture was stirred at rt overnight and then concentrated to a yellow solid (65 mg). This material was combined with additional intermediate (135 mg), dissolved in DMF (7 mL), and added dropwise over 0.5 h to a solution of BOP (331 mg, 0.74 mmol) and DMAP (226 mg, 1.85 mmol) in DCM (75 mL) at 40 °C. The reaction mixture was heated for an additional 0.5 h and then concentrated *in vacuo.* The residual solid was purified by reverse phase HPLC to give 81 mg of white solid. This was combined with 31 mg from a previous run, dissolved in MeOH, and purified by chiral HPLC to give ***(S)*-30** (peak 1, 48 mg, 21%) and ***(R)*-30** (peak 2, 40 mg, 18%). The preparative chromatography conditions were the following: Chiralcel OD column (5 cm ID x 50 cm L, 20 micron, Chiral Technologies, Inc.), 30% (1:1 ethanol/methanol)/70% heptane as eluent, 50 mL/min flow rate, and UV detection at 254 nm. ***(R)*-30** analytical data: MS (ESI) *m/z* 517.1 $(M+H)^+$. ^{1}H NMR (400MHz, CD_3OD) δ 1.24 (t, *J* = 7.5 Hz, 3H), 1.87 (dt, *J* = 6.8, 3.2 Hz, 2H), 2.03-2.14 (m, 1H), 2.27-2.46 (m, 4H), 2.56-2.68 (m, 1H), 2.93 (td, *J* = 7.0, 4.8 Hz, 1H), 3.39 (td, *J* = 14.7, 7.0 Hz, 2H), 3.68-3.76 (m, 2H), 4.15 (d, *J* = 17.1 Hz, 1H), 5.01-5.09 (m, 2H), 6.62 (d, *J* = 1.8 Hz, 1H), 6.65-6.70 (m, 2H), 6.89 (dd, *J* = 8.3, 1.8 Hz, 1H), 6.98-7.03 (m, 1H), 7.07-7.13 (m, 1H), 7.34-7.40 (m, 3H), 7.54 (dd, *J* = 7.7, 2.0 Hz, 1H), 7.76 (d, *J* = 8.3 Hz, 1H). Chiral analytical HPLC retention times: peak 1, 6.95 min; peak 2, 8.17 min using the following chromatography conditions: Chiralcel OD column (4.6 mm ID x 250 mm L, 10 micron, Chiral Technologies, Inc.), 30% (1:1 ethanol/methanol)/70% heptane as eluent, 1 mL/min flow rate, and UV detection at 254 nm.

4-((*R*)-7-Ethanesulfonyl-3,12-dioxo-4,11-diaza-tricyclo[14.2.2.1^{6,10}]henicosa-1(19),6,8,10(21),16(20),17-hexaen-2-ylamino)-benzamidine trifluoroacetic acid salt (*(R)*-31). ***(R)*-30** (30 mg, 0.058 mmol) was dissolved in a solution of hydroxylamine in DMSO (3M, 0.400 mL). The reaction mixture was heated at 70 °C for 3 h. An additional aliquot of hydroxylamine in DMSO (3M, 0.300 mL) was added, and heating was continued for 2 h. The reaction mixture was diluted with ethyl acetate, extracted with water and brine, dried ($MgSO_4$), and concentrated *in vacuo*. Acetic anhydride (0.030 mL, 0.32 mmol) was added to a solution of the residue dissolved in DCM (3 mL). After 30 min at rt, the reaction mixture was concentrated *in vacuo*. The residue was dissolved in MeOH and hydrogenated (50 psi) over 10% palladium on carbon (37 mg) for 2.5 h. The reaction mixture was filtered and concentrated *in vacuo*. The residue was purified by preparative reverse phase HPLC to give ***(R)*-31** (7.3 mg, 19%). MS (ESI) *m/z* 534.0 $(M+H)^+$. ^{1}H NMR (400 MHz, CD_3OD) δ 1.25 (t, *J* = 7.25 Hz, 3H) 2.00-2.16 (m, 1H) 2.27-2.49 (m, 3H) 2.54-2.69 (m, 1H) 2.87-3.00 (m, 1H) 3.32-3.51 (m, 2H) 4.16 (dd, *J* = 16.70, 5.27 Hz, 1H) 5.00-5.14 (m, 2H) 6.63 (d, *J* = 1.76 Hz, 1H) 6.76 (d, *J* = 8.79 Hz, 2H) 6.90 (dd, *J* = 8.57, 1.98 Hz, 1H) 7.02 (dd, *J* = 7.91, 2.20 Hz, 1H) 7.11 (dd, *J* = 7.91, 1.32 Hz, 1H) 7.39 (dd, *J* = 7.91, 1.76 Hz, 1H) 7.52-7.62 (m, 3H) 7.76 (d, *J* = 8.35 Hz, 1H) 8.91 (t, *J* = 5.71 Hz, 1H).

4-(4-Bromo-2-methylphenyl)butanoic acid (33). 9-Borabicyclo[3.3.1]nonane (10 mL, 5 mmol, 0.5N in THF) was treated with methyl but-3-enoate **32** (0.5 g, 5 mmol) dropwise at rt under argon. The reaction mixture was stirred for 3 h at rt. A resealable tube was charged with 5-bromo-2-iodotoluene (1.48 g, 5 mmol), sodium methoxide (853 mg, 15.8 mmol), and dichloro[1,1'-bis(diphenylphosphino)ferrocene] palladium(II) dichloromethane adduct (110 mg, 0.15 mmol) in THF (15 mL). After the hydroboration reaction was complete, it was added to the resealable tube, and the combined reaction mixture was heated to 70 °C for 4 h, then at rt for several days. The reaction mixture was diluted with water and extracted with EtOAc (2x). The combined organics were extracted with water and brine, dried ($MgSO_4$), and concentrated *in vacuo*. The residue was purified by silica gel

chromatography (EtOAc/hexane) to give 513 mg of ester. This material was dissolved in THF (3 mL), MeOH (1.5 mL) and 1 M NaOH (3 mL) and heated for 1 h at 80 °C. Most of the solvent was removed *in vacuo*, 1N HCl (4 mL) was added, and the mixture was extracted with EtOAc (3x). The combined organic layers were washed with brine, dried ($MgSO_4$), and concentrated *in vacuo*. The residue was purified by reverse phase HPLC to give **33** (287 mg, 22%) as a white solid. ^{1}H NMR (400 MHz, $CDCl_3$) δ 1.82-1.96 (m, 2H), 2.28 (s, 3H), 2.42 (t, *J* = 7.25 Hz, 2H), 2.57-2.65 (m, 2H), 6.99 (d, *J* = 7.91 Hz, 1H), 7.23-7.26 (m, 1H), 7.27-7.31 (m, 1H).

4-(4-Bromo-2-methylphenyl)-*N*-(3-cyano-4-(ethylsulfonyl)phenyl)butanamide (34). Oxalyl chloride (0.200 mL, 2.29 mmol) was added dropwise to a solution of **33** (287 mg, 1.12 mmol) in DCM (4 mL) and DMF (1 drop). The reaction mixture was stirred for 4 h, and then concentrated *in vacuo*. The residue was coevaporated with toluene and then dissolved in toluene (10 mL). **19a** (227 mg, 1.08 mmol) was added, and the reaction mixture was heated to reflux for 2 h. The reaction mixture was concentrated *in vacuo*, and the residue was purified by silica gel chromatography (EtOAc/hexane) to give **34** (373 mg, 77%) as an off-white solid. MS (ESI) *m/z* 449.1, 451.1 $(M+H)^+$. ^{1}H NMR (400MHz, $CDCl_3$) δ 1.28-1.35 (m, 3H), 1.95-2.06 (m, 2H), 2.30 (s, 3H), 2.46 (t, *J* = 7.3 Hz, 2H), 2.62-2.70 (m, 2H), 3.35 (q, *J* = 7.5 Hz, 2H), 7.00 (d, *J* = 8.3 Hz, 1H), 7.24 (dd, *J* = 8.1, 2.0 Hz, 1H), 7.28 (s, 1H), 7.78 (s, 1H), 7.90 (dd, *J* = 8.8, 2.2 Hz, 1H), 8.01-8.05 (m, 1H), 8.15 (d, *J* = 2.2 Hz, 1H).

4-(4-(3-Cyano-4-(ethylsulfonyl)phenylamino)-4-oxobutyl)-3-methylphenylboronic acid (35). Using a procedure analogous to that which was used to prepare **7a**, **34** (448 mg, 1.00 mmol) was reacted with bis(neopentyl glycolato)diboron to afford the crude boronic acid. The crude boronic ester (212 mg, 0.44 mmol) was reacted with aqueous NaOH and then purified by silica gel chromatography (MeOH/DCM) to afford **35** (113 mg, 55%). ^{1}H NMR (400 MHz, THF-d_8) δ 1.21 (t, 3H), 1.94-2.04 (m, 2H), 2.40 (t, *J* = 7.25 Hz, 2H), 2.70 (t, *J* = 7.47 Hz, 2H), 3.31 (q, *J* = 7.47 Hz, 2H), 7.01 (s, 2H), 7.08 (d,

J = 7.47 Hz, 1H), 7.53 (d, *J* = 7.47 Hz, 1H), 7.56 (s, 1H), 7.93 (dd, 1H), 7.99 (d, 1H), 1.00 (d, *J* = 2.20 Hz, 1H), 9.66 (s, 1H).

2-(1-Di-*tert*-butoxycarbonylaminoisoquinolin-6-ylamino)-2-(4-(4-(3-cyano-4-(ethylsulfonyl)phenylamino)-4-oxobutyl)-3-methylphenyl)acetic acid (36). Using a procedure analogous to that which was used to prepare **10a**, **35** (113 mg, 0.273 mmol) was reacted with **9** and glyoxylic acid monohydrate to afford **36** (154 mg, 72%) as an off-white solid. MS (ESI) *m/z* 786.3 $(M+H)^+$. ^{1}H NMR (400MHz, DMSO-d_6) δ 1.13 (t, *J* = 7.3 Hz, 3H), 1.30 (s, 18H), 1.74-1.90 (m, 2H), 2.28 (s, 3H), 2.45 (t, *J* = 7.0 Hz, 2H), 2.55-2.64 (m, 2H), 3.39 (q, *J* = 7.3 Hz, 2H), 5.19 (d, *J* = 7.5 Hz, 1H), 6.70 (s, 1H), 7.17 (d, *J* = 7.9 Hz, 2H), 7.27-7.36 (m, 3H), 7.40 (d, *J* = 5.7 Hz, 1H), 7.49 (d, *J* = 9.2 Hz, 1H), 8.03 (d, *J* = 0.9 Hz, 2H), 8.06 (d, *J* = 5.7 Hz, 1H), 8.32 (s, 1H), 10.68 (s, 1H).

(*R*)-2-(1-Amino-isoquinolin-6-ylamino)-7-ethanesulfonyl-20-methyl-4,11-diaza-tricyclo[14.2.2.1^{6,10}]henicosa-1(19),6,8,10(21),16(20),17-hexaene-3,12-dione (*(R)*-37). Using a procedure analogous to that which was used to prepare **23**, **36** (154 mg, 0.263 mmol) was hydrogenated, cyclized, and deprotected to afford racemic **37** (22.6 mg, 12%) as an off-white amorphous solid. NMR and analytical HPLC are consistent with a 1:1 mixture of atropisomers. MS (ESI) *m/z* 572.1 $(M+H)^+$. ^{1}H NMR (400 MHz, CD_3OD) δ 1.19-1.27 (m, 6H), 1.86-1.98 (m, 2H), 2.12-2.21 (m, 1H), 2.28 (t, *J* = 8.97 Hz, 1H), 2.35-2.49 (m, 4H), 2.65-2.75 (m, 1H), 2.87-2.97 (m, 1H), 3.08-3.19 (m, 2H), 3.34-3.45 (m, 4H), 4.10-4.25 (m, 3H), 5.09 (dd, *J* = 17.03, 5.68 Hz, 1H), 5.13 (s, 1H), 5.14 (s, 1H), 6.64-6.71 (m, 4H), 6.80-6.94 (m, 5H), 6.97 (s, 1H), 7.05 (d, *J* = 7.69 Hz, 1H), 7.09-7.17 (m, 2H), 7.29 (d, *J* = 6.96 Hz, 2H), 7.33-7.38 (m, 1H), 7.41-7.46 (m, 1H), 7.47 (s, 1H), 7.76 (d, *J* = 8.42 Hz, 2H), 8.01 (d, *J* = 4.03 Hz, 1H), 8.02-8.05 (m, 1H), 8.89 (t, *J* = 5.86 Hz, 1H), 8.95 (t, *J* = 6.04 Hz, 1H).

A solution of racemic **37** (0.100 g, 0.146 mmol) in methanol was purified by chiral supercritical fluid chromatography to give ***(S)*-37** (peak 1, 28 mg, 34%) and ***(R)*-37** (peak 2, 29 mg, 35%). The chromatography conditions were the following: Chiralpak AS column (3.0 cm ID x 25 cm L, 10 micron,

Chiral Technologies, Inc.), 75% CO_2/25% methanol/0.1% diethylamine as eluent, 100 bar, 40 °C, 65 mL/min flow rate, and UV detection at 220 nm. ***(R)*-37** analytical data: MS (ESI) *m/z* 572.10 $(M+H)^+$. ^1H NMR (400 MHz, CD_3OD) δ 1.21-1.33 (m, 3H) 1.87-2.00 (m, 1H) 2.26 (s, 1H) 2.37-2.54 (m, 5H) 2.66-2.76 (m, 1H) 2.89-3.00 (m, 1H) 3.08-3.18 (m, 1H) 3.33-3.51 (m, 3H) 4.23 (t, *J* = 17.36 Hz, 1H) 4.99-5.12 (m, 2H) 6.55-6.62 (m, 1H) 6.64-6.69 (m, 1H) 6.69-6.76 (m, 1H) 6.85-6.95 (m, 1H) 6.97-7.10 (m, 2H) 7.30-7.36 (m, 2H) 7.38-7.51 (m, 2H) 7.77 (d, *J* = 8.79 Hz, 1H) 7.81-7.88 (m, 1H), mixture of two atropisomers. Chiral analytical HPLC retention times: peak 1, 20.00 min; peak 2, 24.99 min using the following chromatography conditions: Whelk-01 (R,R) column (4.6 mm ID x 250 mm L, 10 micron.), 40% (1:1 ethanol/methanol)/60% heptane/0.1% diethylamine as eluent, 2 mL/min flow rate, and UV detection at 264 nm.

Supporting Information. Analytical data and selected experimental procedures for compounds **3-5**, **15, 16**, **(*R*)-24**, and **(*rac*)-25**, and crystallographic refinement statistics. This material is available free of charge via the Internet at http://pubs.acs.org.

PDB ID Codes. 4ZXX and 4ZXY

Abbreviations Used. TF, tissue factor; FVIIa, coagulation factor VIIa; FIXa, coagulation factor IXa; FXa, coagulation factor Xa; APC, activated protein C; tissue kall., tissue kallikrein-1; AIQ, aminoisoquinoline; BZD, benzamidine; EC_{2x}, effective concentration that doubles clotting time.

Acknowledgement. The authors thank Peter Glunz, Dean Wacker, and Don Pinto for critical review of this manuscript, We thank Steven Sheriff for helping to prepare the coordinates and data of compounds **1** and **(*R*)-4** and depositing them in the PDB, Yanfeng Zhang for preparation of compounds **15** and **16,** Jeff Bozarth, Randi Brown, Tara Peterson, and Mojgan Abousleiman for obtaining the enzyme inhibition data, and Frank Barbera and Yiming Wu for obtaining the clotting assay data.

References

1. Mackman, N.; Tilley, R. E.; Key, N. S. Role of the extrinsic pathway of blood coagulation in hemostasis and thrombosis. *Arterioscler. Thromb. Vasc. Biol.* **2007,** 27, 1687-1693.

2. Banner, D. W.; D'Arcy, A.; Chene, C.; Winkler, F. K.; Guha, A.; Konigsberg, W. H.; Nemerson, Y.; Kirchhofer, D. The crystal structure of the complex of blood coagulation factor VIIa with soluble tissue factor. *Nature* **1996,** 380, 41-46.

3. Harker, L. A.; Hanson, S. R.; Wilcox, J. N.; Kelly, A. B. Antithrombotic and antilesion benefits without hemorrhagic risks by inhibiting tissue factor pathway. *Haemostasis* **1996,** 26, Suppl. 1, 76-82.

4. Golino, P.; Ragni, M.; Cirillo, P.; D'Andrea, D.; Scognamiglio, A.; Ravera, A.; Buono, C.; Ezban, M.; Corcione, N.; Vigorito, F.; Condorelli, M.; Chiariello, M. Antithrombotic effects of recombinant human, active site-blocked factor VIIa in a rabbit model of recurrent arterial thrombosis. *Circ. Res.* **1998,** 82, 39-46.

5. Suleymanov, O. D.; Szalony, J. A.; Salyers, A. K.; Lachance, R. M.; Parlow, J. J.; South, M. S.; Wood, R. S.; Nicholson, N. S. Pharmacological interruption of acute thrombus formation with minimal hemorrhagic complications by a small molecule tissue factor/factor VIIa inhibitor: Comparison to factor Xa and thrombin inhibition in a nonhuman primate thrombosis model. *J. Pharmacol. Exp. Ther.* **2003,** 306, 1115-1121.

6. Szalony, J. A.; Suleymanov, O. D.; Salyers, A. K.; Panzer-Knodle, S. G.; Blom, J. D.; LaChance, R. M.; Case, B. L.; Parlow, J. J.; South, M. S.; Wood, R. S.; Nicholson, N. S. Administration of a small molecule tissue factor/factor VIIa inhibitor in a non-human primate thrombosis model of venous thrombosis: effects on thrombus formation and bleeding time. *Thromb. Res.* **2003,** 112, 167-174.

7. Salyers, A. K.; Szalony, J. A.; Suleymanov, O. D.; Parlow, J. J.; Wood, R. S.; South, M. S.; Nicholson, N. S. Assessment of bleeding propensity in non-human primates by combination of selective tissue factor/VIIa inhibition and aspirin compared to warfarin and aspirin treatment. *Pharmacology* **2004,** 70, 100-106.

8. Olivero, A. G.; Eigenbrot, C.; Goldsmith, R.; Robarge, K.; Artis, D. R.; Flygare, J.; Rawson, T.; Sutherlin, D. P.; Kadkhodayan, S.; Beresini, M.; Elliott, L. O.; DeGuzman, G. G.; Banner, D. W.; Ultsch, M.; Marzec, U.; Hanson, S. R.; Refino, C.; Bunting, S.; Kirchhofer, D. A selective, slow binding inhibitor of factor VIIa binds to a nonstandard active site conformation and attenuates thrombus formation in vivo. *J. Biol. Chem.* **2005,** 280, 9160-9169.

9. Young, W. B.; Mordenti, J.; Torkelson, S.; Shrader, W. D.; Kolesnikov, A.; Rai, R.; Liu, L.; Hu, H.; Leahy, E. M.; Green, M. J.; Sprengeler, P. A.; Katz, B. A.; Yu, C.; Janc, J. W.; Elrod, K. C.; Marzec, U. M.; Hanson, S. R. Factor VIIa inhibitors: Chemical optimization, preclinical pharmacokinetics, pharmacodynamics, and efficacy in an arterial baboon thrombosis model. *Bioorg. Med. Chem. Lett.* **2006,** 16, 2037-2041.

10. Zbinden, K. G.; Banner, D. W.; Hilpert, K.; Himber, J.; Lave, T.; Riederer, M. A.; Stahl, M.; Tschopp, T. B.; Obst-Sander, U. Dose-dependent antithrombotic activity of an orally active tissue factor/factor VIIa inhibitor without concomitant enhancement of bleeding propensity. *Bioorg. Med. Chem.* **2006,** 14, 5357-5369.

11. Arnold, C. S.; Parker, C.; Upshaw, R.; Prydz, H.; Chand, P.; Kotian, P.; Bantia, S.; Babu, Y. S. The antithrombotic and anti-inflammatory effects of BCX-3607, a small molecule tissue factor/factor VIIa inhibitor. *Thromb. Res.* **2006,** 117, 343-349.

12. Wong, P. C.; Luettgen, J. M.; Rendina, A. R.; Kettner, C. A.; Xin, B.; Knabb, R. M.; Wexler, R. R.; Priestley, E. S. BMS-593214, an active site-directed factor VIIa inhibitor: enzyme kinetics, antithrombotic and antihemostatic studies. *Thromb. Haemostasis* **2010,** 104, 261-269.

13. Lee, A.; Agnelli, G.; Buller, H.; Ginsberg, J.; Heit, J.; Rote, W.; Vlasuk, G.; Costantini, L.; Julian, J.; Comp, P.; van der Meer, J.; Piovella, F.; Raskob, G.; Gent, M. Dose-response study of recombinant factor VIIa/tissue factor inhibitor recombinant nematode anticoagulant protein c2 in prevention of postoperative venous thromboembolism in patients undergoing total knee replacement. *Circulation* **2001,** 104, 74-78.

14. Moons, A. H. M.; Peters, R. J. G.; Bijsterveld, N. R.; Piek, J. J.; Prins, M. H.; Vlasuk, G. P.; Rote, W. E.; Buller, H. R. Recombinant nematode anticoagulant protein c2, an inhibitor of the tissue factor/factor VIIa complex, in patients undergoing elective coronary angioplasty. *J. Am. Coll. Cardiol.* **2003,** 41, 2147-2153.

15. Giugliano, R. P.; Wiviott, S. D.; Stone, P. H.; Simon, D. I.; Schweiger, M. J.; Bouchard, A.; Leesar, M. A.; Goulder, M. A.; Deitcher, S. R.; McCabe, C. H.; Braunwald, E. Recombinant nematode anticoagulant protein c2 in patients with non-ST-segment elevation acute coronary syndrome: the ANTHEM-TIMI-32 trial. *J. Am. Coll. Cardiol.* **2007,** 49, 2398-407.

16. Young, W. B.; Kolesnikov, A.; Rai, R.; Sprengeler, P. A.; Leahy, E. M.; Shrader, W. D.; Sangalang, J.; Burgess-Henry, J.; Spencer, J.; Elrod, K.; Cregar, L. Optimization of a screening lead for factor VIIa/TF. *Bioorg. Med. Chem. Lett.* **2001,** 11, 2253-2256.

17. Riggs, J. R.; Kolesnikov, A.; Hendrix, J.; Young, W. B.; Shrader, W. D.; Vijaykumar, D.; Stephens, R.; Liu, L.; Pan, L.; Mordenti, J.; Green, M. J.; Sukbuntherng, J. Factor VIIa inhibitors: A prodrug strategy to improve oral bioavailability. *Bioorg. Med. Chem. Lett.* **2006,** 16, 2224-2228.

18. Kolesnikov, A.; Rai, R.; Young, W. B.; Mordenti, J.; Liu, L.; Torkelson, S.; Shrader, W. D.; Leahy, E. M.; Hu, H.; Gjerstad, E.; Janc, J.; Katz, B. A.; Sprengeler, P. A. Factor VIIa inhibitors: improved pharmacokinetic parameters. *Bioorg. Med. Chem. Lett.* **2006,** 16, 2243-2246.

19. Rai, R.; Kolesnikov, A.; Sprengeler, P. A.; Torkelson, S.; Ton, T.; Katz, B. A.; Yu, C.; Hendrix, J.; Shrader, W. D.; Stephens, R.; Cabuslay, R.; Sanford, E.; Young, W. B. Discovery of novel heterocyclic factor VIIa inhibitors. *Bioorg. Med. Chem. Lett.* **2006,** 16, 2270-2273.

20. Riggs, J. R.; Hu, H.; Kolesnikov, A.; Leahy, E. M.; Wesson, K. E.; Shrader, W. D.; Vijaykumar, D.; Wahl, T. A.; Tong, Z.; Sprengeler, P. A.; Green, M. J.; Yu, C.; Katz, B. A.; Sanford, E.; Nguyen, M.; Cabuslay, R.; Young, W. B. Novel 5-azaindole factor VIIa inhibitors. *Bioorg. Med. Chem. Lett.* **2006,** 16, 3197-3200.

21. Vijaykumar, D.; Rai, R.; Shaghafi, M.; Ton, T.; Torkelson, S.; Leahy, E. M.; Riggs, J. R.; Hu, H.; Sprengeler, P. A.; Shrader, W. D.; O'Bryan, C.; Cabuslay, R.; Sanford, E.; Gjerstadt, E.; Liu, L.; Sukbuntherng, J.; Young, W. B. Efforts toward oral bioavailability in factor VIIa inhibitors. *Bioorg. Med. Chem. Lett.* **2006,** 16, 3829-3832.

22. Hu, H.; Kolesnikov, A.; Riggs, J. R.; Wesson, K. E.; Stephens, R.; Leahy, E. M.; Shrader, W. D.; Sprengeler, P. A.; Green, M. J.; Sanford, E.; Nguyen, M.; Gjerstad, E.; Cabuslay, R.; Young, W. B. Potent 4-amino-5-azaindole factor VIIa inhibitors. *Bioorg. Med. Chem. Lett.* **2006,** 16, 4567-4570.

23. Zbinden, K. G.; Banner, D. W.; Ackermann, J.; D'Arcy, A.; Kirchhofer, D.; Ji, Y.-H.; Tschopp, T. B.; Wallbaum, S.; Weber, L. Design of selective phenylglycine amide tissue factor/factor VIIa inhibitors. *Bioorg. Med. Chem. Lett.* **2005,** 15, 817-822.

24. Zbinden, K. G.; Obst-Sander, U.; Hilpert, K.; Kuehne, H.; Banner, D. W.; Boehm, H.-J.; Stahl, M.; Ackermann, J.; Alig, L.; Weber, L.; Wessel, H. P.; Riederer, M. A.; Tschopp, T. B.; Lave, T. Selective and orally bioavailable phenylglycine tissue factor/factor VIIa inhibitors. *Bioorg. Med. Chem. Lett.* **2005,** 15, 5344-5352.

25. Glunz, P. W.; Zhang, X.; Zou, Y.; Delucca, I.; Nirschl, A. H.; Cheng, X.; Weigelt, C. A.; Cheney, D. L.; Wei, A.; Anumula, R.; Luettgen, J. M.; Rendina, A. R.; Harpel, M.; Luo, G.; Knabb, R.; Wong, P. C.; Wexler, R. R.; Priestley, E. S. Nonbenzamidine acylsulfonamide tissue factor-factor VIIa inhibitors. *Bioorg. Med. Chem. Lett.* **2013,** 23, 5244-5248.

26. Zhang, X.; Jiang, W.; Jacutin-Porte, S.; Glunz, P. W.; Zou, Y.; Cheng, X.; Nirschl, A. H.; Wurtz, N. R.; Luettgen, J. M.; Rendina, A. R.; Luo, G.; Harper, T. M.; Wei, A.; Anumula, R.; Cheney, D. L.; Knabb, R. M.; Wong, P. C.; Wexler, R. R.; Priestley, E. S. Design and synthesis of phenylpyrrolidine phenylglycinamides as highly potent and selective TF-FVIIA inhibitors. *ACS Med. Chem. Lett.* **2014,** 5, 188-192.

27. South, M. S.; Case, B. L.; Wood, R. S.; Jones, D. E.; Hayes, M. J.; Girard, T. J.; Lachance, R. M.; Nicholson, N. S.; Clare, M.; Stevens, A. M.; Stegeman, R. A.; Stallings, W. C.; Kurumbail, R. G.;

Parlow, J. J. Structure-based drug design of pyrazinone antithrombotics as selective inhibitors of the tissue factor VIIa complex. *Bioorg. Med. Chem. Lett.* **2003,** 13, 2319-2325.

28. Parlow, J. J.; Case, B. L.; Dice, T. A.; Fenton, R. L.; Hayes, M. J.; Jones, D. E.; Neumann, W. L.; Wood, R. S.; Lachance, R. M.; Girard, T. J.; Nicholson, N. S.; Clare, M.; Stegeman, R. A.; Stevens, A. M.; Stallings, W. C.; Kurumbail, R. G.; South, M. S. Design, parallel synthesis, and crystal structures of pyrazinone antithrombotics as selective inhibitors of the tissue factor VIIa complex. *J. Med. Chem.* **2003,** 46, 4050-4062.

29. Parlow, J. J.; Kurumbail, R. G.; Stegeman, R. A.; Stevens, A. M.; Stallings, W. C.; South, M. S. Design, synthesis, and crystal structure of selective 2-pyridone tissue factor VIIa inhibitors. *J. Med. Chem.* **2003,** 46, 4696-4701.

30. Schweitzer, B., A.; Neumann, W., L.; Rahman, H., K.; Kusturin, C., L.; Sample, K., R.; Poda, G., I.; Kurumbail, R., G.; Stevens, A., M.; Stegeman, R., A.; Stallings, W., C.; South, M., S. Structure-based design and synthesis of pyrazinones containing novel P1 'side pocket' moieties as inhibitors of TF/VIIa. *Bioorg. Med. Chem. Lett.* **2005,** 15, 3006-11.

31. Zhang, X.; Glunz, P. W.; Jiang, W.; Schmitt, A.; Newman, M.; Barbera, F. A.; Bozarth, J. M.; Rendina, A. R.; Wei, A.; Wen, X.; Rossi, K. A.; Luettgen, J. M.; Wong, P. C.; Knabb, R. M.; Wexler, R. R.; Priestley, E. S. Design and synthesis of bicyclic pyrazinone and pyrimidinone amides as potent TF-FVIIa inhibitors. *Bioorg. Med. Chem. Lett.* **2013,** 23, 1604-1607.

32. Priestley, E. S.; DeLucca, I.; Zhou, J.; Zhou, J.; Saiah, E.; Stanton, R.; Robinson, L.; Luettgen, J. M.; Wei, A.; Wen, X.; Knabb, R. M.; Wong, P. C.; Wexler, R. R. Discovery and gram-scale synthesis of BMS-593214, a potent, selective FVIIa inhibitor. *Bioorg. Med. Chem. Lett.* **2013,** 23, 2432-2435.

33. Kohrt, J. T.; Filipski, K. J.; Cody, W. L.; Cai, C.; Dudley, D. A.; Van Huis, C. A.; Willardsen, J. A.; Rapundalo, S. T.; Saiya-Cork, K.; Leadley, R. J.; Narasimhan, L.; Zhang, E.; Whitlow, M.; Adler, M.; McLean, K.; Chou, Y.-L.; McKnight, C.; Arnaiz, D. O.; Shaw, K. J.; Light, D. R.; Edmunds, J. J.

The discovery of fluoropyridine-based inhibitors of the Factor VIIa/TF complex. *Bioorg. Med. Chem. Lett.* **2005,** 15, 4752-4756.

34. Kohrt, J. T.; Filipski, K. J.; Cody, W. L.; Cai, C.; Dudley, D. A.; Van Huis, C. A.; Willardsen, J. A.; Narasimhan, L. S.; Zhang, E.; Rapundalo, S. T.; Saiya-Cork, K.; Leadley, R. J.; Edmunds, J. J. The discovery of fluoropyridine-based inhibitors of the factor VIIa/TF complex-Part 2. *Bioorg. Med. Chem. Lett.* **2006,** 16, 1060-1064.

35. Klingler, O.; Matter, H.; Schudok, M.; Bajaj, S. P.; Czech, J.; Lorenz, M.; Nestler, H. P.; Schreuder, H.; Wildgoose, P. Design, synthesis, and structure-activity relationship of a new class of amidinophenylurea-based factor VIIa inhibitors. *Bioorg. Med. Chem. Lett.* **2003,** 13, 1463-1467.

36. Klingler, O.; Matter, H.; Schudok, M.; Donghi, M.; Czech, J.; Lorenz, M.; Nestler, H. P.; Szillat, H.; Schreuder, H. Structure-based design of amidinophenylurea-derivatives for factor VIIa inhibition. *Bioorg. Med. Chem. Lett.* **2004,** 14, 3715-3720.

37. Kohrt, J. T.; Filipski, K. J.; Rapundalo, S. T.; Cody, W. L.; Edmunds, J. J. An efficient synthesis of 2-[3-(4-amidinophenylcarbamoyl)naphthalen-2-yl]-5-[(2,2-methylpropyl)carbamoyl]benzoic acid: a factor VIIa inhibitor discovered by the Ono Pharmaceutical Company. *Tetrahedron Lett.* **2000,** 41, 6041-6044.

38. Miura, M.; Seki, N.; Koike, T.; Ishihara, T.; Niimi, T.; Hirayama, F.; Shigenaga, T.; Sakai-Moritani, Y.; Kawasaki, T.; Sakamoto, S.; Okada, M.; Ohta, M.; Tsukamoto, S.-I. Potent and selective TF/FVIIa inhibitors containing a neutral P1 ligand. *Bioorg. Med. Chem.* **2006,** 14, 7688-7705.

39. Miura, M.; Seki, N.; Koike, T.; Ishihara, T.; Niimi, T.; Hirayama, F.; Shigenaga, T.; Sakai-Moritani, Y.; Tagawa, A.; Kawasaki, T.; Sakamoto, S.; Okada, M.; Ohta, M.; Tsukamoto, S.-i. Design, synthesis and biological activity of selective and orally available TF/FVIIa complex inhibitors containing non-amidine P1 ligands. *Bioorg. Med. Chem.* **2007,** 15, 160-173.

40. Kotian, P. L.; Krishnan, R.; Rowland, S.; El-Kattan, Y.; Saini, S. K.; Upshaw, R.; Bantia, S.; Arnold, S.; Sudhakar, B. Y.; Chand, P. Design, parallel synthesis, and crystal structures of biphenyl

antithrombotics as selective inhibitors of tissue factor FVIIa complex. Part 1: Exploration of S2 pocket pharmacophores. *Bioorg. Med. Chem.* **2009,** 17, 3934-3958.

41. Bolton, S. A.; Sutton, J. C.; Anumula, R.; Bisacchi, G. S.; Jacobson, B.; Slusarchyk, W. A.; Treuner, U. D.; Wu, S. C.; Zhao, G.; Pi, Z.; Sheriff, S.; Smirk, R. A.; Bisaha, S.; Cheney, D. L.; Wei, A.; Schumacher, W. A.; Hartl, K. S.; Liu, E.; Zahler, R.; Seiler, S. M. Discovery of nonbenzamidine factor VIIa inhibitors using a biaryl acid scaffold. *Bioorg. Med. Chem. Lett.* **2013,** 23, 5239-5243.

42. Sagi, K.; Fujita, K.; Sugiki, M.; Takahashi, M.; Takehana, S.; Tashiro, K.; Kayahara, T.; Yamanashi, M.; Fukuda, Y.; Oono, S.; Okajima, A.; Iwata, S.; Shoji, M.; Sakurai, K. Optimization of a coagulation factor VIIa inhibitor found in factor Xa inhibitor library. *Bioorg. Med. Chem.* **2005,** 13, 1487-1496.

43. Glunz, P. W.; Cheng, X.; Cheney, D. L.; Weigelt, C. A.; Wei, A.; Luettgen, J. M.; Wong, P. C.; Wexler, R. R.; Priestley, E. S. Design and synthesis of potent, selective phenylimidazole-based FVIIa inhibitors. *Bioorg. Med. Chem. Lett.* **2015**, in press.

44. Priestley, E. S. Tissue factor-fVIIa inhibition: update on an unfinished quest for a novel oral antithrombotic. *Drug Discov. Today* **2014,** 19, 1440-1444.

45. We use the nomenclature of Schechter and Berger to describe specific regions of the protease active site and, by analogy to peptide substrates, the inhibitor. Schechter, I.; Berger, A. On the size of the active site in proteases. I. Papain. Biochem. Biophys. Res. Commun. 1967, 27, 157-62.

46. Cheney, D. L.; Bozarth, J. M.; Metzler, W. J.; Morin, P. E.; Mueller, L.; Newitt, J. A.; Nirschl, A. H.; Rendina, A. R.; Tamura, J. K.; Wei, A.; Wen, X.; Wurtz, N. R.; Seiffert, D. A.; Wexler, R. R.; Priestley, E. S. Discovery of novel P1 groups for coagulation factor VIIa inhibition using fragment-based screening. *J. Med. Chem.* **2015,** 58, 2799-2808.

47. Quan, M. L.; Wexler, R. R. The design and synthesis of noncovalent Factor Xa inhibitors. *Curr. Top. Med. Chem.* **2001,** 1, 137-149.

48. Lam, P. Y. S.; Clark, C. G.; Li, R.; Pinto, D. J. P.; Orwat, M. J.; Galemmo, R. A.; Fevig, J. M.; Teleha, C. A.; Alexander, R. S.; Smallwood, A. M.; Rossi, K. A.; Wright, M. R.; Bai, S. A.; He, K.; Luettgen, J. M.; Wong, P. C.; Knabb, R. M.; Wexler, R. R. Structure-based design of novel guanidine/benzamidine mimics: potent and orally bioavailable factor Xa inhibitors as novel anticoagulants. *J. Med. Chem.* **2003,** 46, 4405-4418.

49. Pinto, D. J. P.; Galemmo, R. A.; Quan, M. L.; Orwat, M. J.; Clark, C.; Li, R.; Wells, B.; Woerner, F.; Alexander, R. S.; Rossi, K. A.; Smallwood, A.; Wong, P. C.; Luettgen, J. M.; Rendina, A. R.; Knabb, R. M.; He, K.; Wexler, R. R.; Lam, P. Y. S. Discovery of potent, efficacious, and orally bioavailable inhibitors of blood coagulation factor Xa with neutral P1 moieties. *Bioorg. Med. Chem. Lett.* **2006,** 16, 5584-5589.

50. Jackson, S.; DeGrado, W.; Dwivedi, A.; Parthasarathy, A.; Higley, A.; Krywko, J.; Rockwell, A.; Markwalder, J.; Wells, G.; et al. Template-Constrained Cyclic Peptides: Design of High-Affinity Ligands for GPIIb/IIIa. *J. Am. Chem. Soc.* **1994,** 116, 3220-30.

51. Cherney, R. J.; Wang, L.; Meyer, D. T.; Xue, C. B.; Wasserman, Z. R.; Hardman, K. D.; Welch, P. K.; Covington, M. B.; Copeland, R. A.; Arner, E. C.; DeGrado, W. F.; Decicco, C. P. Macrocyclic amino carboxylates as selective MMP-8 inhibitors. *J. Med. Chem.* **1998,** 41, 1749-51.

52. Kim, Y.-K.; Arai, M. A.; Arai, T.; Lamenzo, J. O.; Dean, E. F., III; Patterson, N.; Clemons, P. A.; Schreiber, S. L. Relationship of Stereochemical and Skeletal Diversity of Small Molecules to Cellular Measurement Space. *J. Am. Chem. Soc.* **2004,** 126, 14740-14745.

53. Driggers, E. M.; Hale, S. P.; Lee, J.; Terrett, N. K. The exploration of macrocycles for drug discovery-an underexploited structural class. *Nat. Rev. Drug Discov.* **2008,** 7, 608-24.

54. Marsault, E.; Peterson, M. L. Macrocycles are great cycles: applications, opportunities, and challenges of synthetic macrocycles in drug discovery. *J. Med. Chem.* **2011,** 54, 1961-2004.

55. Vendeville, S.; Cummings, M. D. Synthetic macrocycles in small-molecule drug discovery. *Annu. Rep. Med. Chem.* **2013,** 48, 371-386.

56. Giordanetto, F.; Kihlberg, J. Macrocyclic drugs and clinical candidates: what can medicinal chemists learn from their properties? *J Med Chem* **2014,** 57, 278-95.

57. Macias, J.; Neukam, K.; Merchante, N.; Pineda, J. A. Latest pharmacotherapy options for treating hepatitis C in HIV-infected patients. *Expert Opin. Pharmacother.* **2014,** 15, 1837-1848.

58. The electron density within 2 Å of compound 1 is depicted in red using the initial electron density Fo-Fc map contoured at 3 r.m.s.d.

59. Molecular graphics were generated using the PyMOL Molecular Graphics System, Version 1.5.0.4 Schrödinger, LLC.

60. Discover_3, Accelrys, Inc.: San Diego, CA.

61. The pKa of 2, 6-diaminoisoquinoline was estimated to be 9.3 and the pKa of 4-aminobenzamidine was estimated to be 13.4 using the Turbomole and COSMOtherm software packages. TURBOMOLE V6.2 2010, A development of University of Karlsruhe and Forschungszentrum Karlsruhe GmbH, 1989-2007,TURBOMOLE GmbH, since 2007; available from http://www.turbomole.com. COSMOtherm version C3.0 revision 13.01, COSMOlogic GmbH & Co. KG Imbacher Weg 46, 51379 , Leverkusen Germany.

62. Petasis, N. A.; Goodman, A.; Zavialov, I. A. A new synthesis of α-arylglycines from aryl boronic acids. *Tetrahedron* **1997,** 53, 16463-16470.

63. Ishiyama, T.; Murata, M.; Miyaura, N. Palladium(0)-Catalyzed Cross-Coupling Reaction of Alkoxydiboron with Haloarenes: A Direct Procedure for Arylboronic Esters. *J. Org. Chem.* **1995,** 60, 7508-10.

64. Brown, H. C.; Prasad, J. V. N. V. Chiral synthesis via organoboranes. 9. Crystalline chelates from borinic and boronic esters. A simple procedure for upgrading borinates and boronates to materials approaching 100% optical purity. *J. Org. Chem.* **1986,** 51, 4526-30.

65. Esteban, G.; Lopez-Sanchez, M. A.; Martinez, M. E.; Plumet, J. A convenient procedure for the synthesis of 1-tetralone derivatives using a Suzuki coupling-Friedel-Crafts acylation sequence. *Tetrahedron* **1998,** 54, 197-212.

66. The electron density within 2 Å of compound (R)-4 is depicted in red using the initial electron density Fo-Fc map contoured at 3 r.m.s.d.

67. Relative atomic coordinates for the crystallographic structures of **1** and **(*R*)-4** complexed with factor VIIa have been deposited in the PDB; their deposition numbers are 4ZXX and 4ZXY, respectively.

68. Otwinowski, Z.; Minor, W. Processing of x-ray diffraction data collected in oscillation mode. In *Methods Enzymol.*, Academic Press, Inc.: New York, NY, 1997; Vol. 276 (Macromolecular Crystallography part A), pp 307-326.

69. Brünger, A. T.; Kuriyan, J.; Karplus, M. Crystallographic R factor refinement by molecular dynamics. *Science* **1987,** 235, 458-460.

70. Emsley, P.; Lohkamp, B.; Scott, W. G.; Cowtan, K. Features and development of Coot. *Acta Crystallogr., Sect. D: Biol. Crystallogr.* **2010,** 66, 486-501.

71. Hwang, M. J.; Ni, X.; Waldman, M.; Ewig, C. S.; Hagler, A. T. Derivation of class II force fields. VI. Carbohydrate compounds and anomeric effects. *Biopolymers* **1998,** 45, 435-468.

72. Maple, J. R.; Hwang, M. J.; Jalkanen, K. J.; Stockfisch, T. P.; Hagler, A. T. Derivation of class II force fields. V. Quantum force field for amides, peptides, and related compounds. *J. Comput. Chem.* **1998,** 19, 430-458.

73. Maple, J. R.; Hwang, M. J.; Stockfisch, T. P.; Hagler, A. T. Derivation of Class II force fields. III. Characterization of a quantum force field for alkanes. *Isr. J. Chem.* **1994,** 34, 195-231.

74. Hwang, M. J.; Stockfisch, T. P.; Hagler, A. T. Derivation of Class II Force Fields. 2. Derivation and Characterization of a Class II Force Field, CFF93, for the Alkyl Functional Group and Alkane Molecules. *J. Am. Chem. Soc.* **1994,** 116, 2515-25.

75. Maple, J. R.; Hwang, M. J.; Stockfisch, T. P.; Dinur, U.; Waldman, M.; Ewig, C. S.; Hagler, A. T. Derivation of Class II force fields. I. Methodology and quantum force field for the alkyl function group and alkane molecules. *J. Comput. Chem.* **1994,** 15, 162-82.

76. MacroModel, version 9.0; Schrödinger, LLC: New York, NY, 2005.

77. Liljefors, T.; Bostrom, J.; Norrby, P.-O. Conformational energies of protein-bound ligands. *Alfred Benzon Symp.* **1998,** 42, 246-263.

78. Bostrom, J.; Norrby, P.-O.; Liljefors, T. Conformational energy penalties of protein-bound ligands. *J. Comput.-Aided Mol. Des.* **1998,** 12, 383-396.

79. Jaguar, version 6.0; Schrödinger, LLC: New York, NY, 2005.

Table of Contents graphic